pubs.acs.org/acschemicalbiology

Article

Split NeissLock with Spy-Acceleration Arms Mammalian Proteins for Anhydride-Mediated Cell Ligation

Sheryl Y. T. Lim,[‖] Anthony H. Keeble,[‖] and Mark R. Howarth*

Cite This: https://doi.org/10.1021/acschembio.5c00515

Read Online

ACCESS | Metrics & More | Article Recommendations | Supporting Information

ABSTRACT: Reactive functional groups may be incorporated into proteins or may emerge from natural amino acids in exceptional architectures. Anhydride formation is triggered by calcium in the self-processing module (SPM) of *Neisseria meningitidis* FrpC, which we previously engineered for "NeissLock" ligation to an unmodified target protein. Here, we explored bacterial diversity, discovering a related module with ultrafast anhydride formation. We dissected this swift SPM to generate a split NeissLock system, providing a second layer of control of anhydride generation: first mixing N- and C-terminal NeissLock moieties and second adding millimolar amounts of calcium. Split NeissLock generated a minimal fusion tag, permitting binder expression in mammalian cells with complex post-translational modifications and avoiding self-cleavage while transiting the calcium-rich secretory pathway. Employing spontaneous amidation between SpyTag003 and SpyCatcher003, we dramatically accelerated split NeissLock reconstitution, allowing a rapid high-yield reaction to naturally occurring targets. We established a specific covalent reaction to endogenous Epidermal Growth Factor Receptor using split NeissLock via Transforming Growth Factor-α secreted from mammalian cells. Modular ligation was demonstrated on living cells through site-specific coupling of the clot-busting enzyme tissue plasminogen activator or a computationally designed cytokine. Split NeissLock provides a modular architecture to generate highly reactive functionality, with inducibility and simple genetic encoding for enhanced cellular modification.

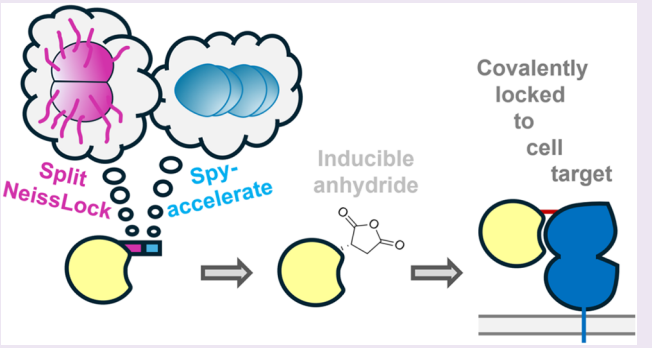

INTRODUCTION

Covalent coupling brings new possibilities for robust and long-lasting assemblies, useful for biotransformation,[1] diagnostics,[2] vaccines,[3] and cell therapies.[4,5] Highly reactive electrophiles such as acid anhydrides and *N*-hydroxysuccinimides are regularly used for coupling to proteins, including for fluorescent labeling and proteomics.[6,7] Such classic reactants produce broad, uncontrolled reaction.[6] For covalent coupling to untagged endogenous proteins with more specificity, electrophiles of lower reactivity, such as acrylamide,[8,9] chloroacetyl,[10] or Sulfur(VI) Fluoride Exchange (SuFEx) probes, are more commonly used.[11] Employing these weak electrophiles to direct protein−protein ligation may be limited by the cost and complexity of attaching these electrophiles through a separate reaction (e.g., coupling through cysteine)[8,9] or through noncanonical amino acid mutagenesis.[12−14] Hence, we have been exploring ways to incorporate electrophiles into proteins using only the standard 20 amino acids.[15,16] *Neisseria meningitidis* FrpC contains a self-processing module (SPM) that, upon binding calcium, cleaves at the aspartate-proline (D-P) peptide bond, releasing SPM to reveal an aspartic anhydride (Figure 1A).[15,16] Aspartic anhydride is a highly reactive electrophile, susceptible to rapid reaction with water.[6] Developing control of this anhydride's reactivity in diverse contexts would create new opportunities for molecular engineering.

We previously redirected anhydrides for what we termed NeissLock coupling[17] (Figure 1B), taking advantage of the feature that any protein can be N-terminal to SPM.[16] In NeissLock, a binding protein that interacts noncovalently with a target is fused with SPM (Figure 1B). The two components are then mixed to form a noncovalent complex, before cleavage at aspartate-proline is initiated with calcium. The resulting anhydride can then react with nearby nucleophiles on the target protein, creating an irreversible covalent complex.[17] Here, we enhance the NeissLock system by identifying a faster SPM. We then split the SPM so that NeissLock may be performed on proteins expressed in mammalian cells. Through the use of SpyTag/SpyCatcher, we accelerate the reconstitution of the split SPM system. Then, we demonstrate the

Received: July 3, 2025
Revised: August 11, 2025
Accepted: August 25, 2025

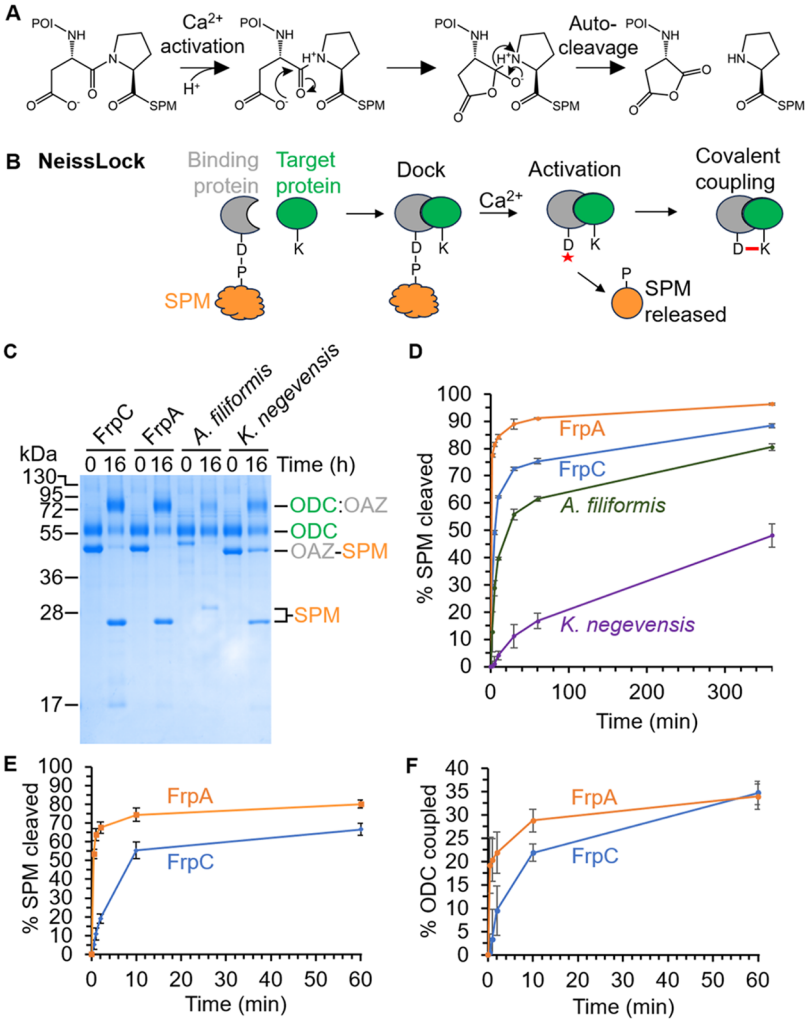

Figure 1. Identifying an ultrafast self-processing module (SPM). (A) SPM undergoes autoproteolysis at Asp-Pro, generating an anhydride. POI is the protein of interest. (B) Schematic of NeissLock. A binding protein genetically fused to SPM docks with a target protein. Upon adding calcium, an anhydride (marked by the red star) is generated on the binding protein, releasing SPM, and enabling covalent coupling to a nucleophile (e.g., lysine, K) on the target. The red line represents an isopeptide bond. (C) Reactivity of SPM homologues. Incubation of different versions of 5 μM OAZ-SPM with 5 μM ODC for 0 or 16 h was done with 10 mM calcium at 37 °C, before SDS−PAGE/Coomassie analysis. A colon indicates covalent coupling. (D) Time course for SPM cleavage. 5 μM OAZ-SPM was mixed with 5 μM ODC for varying times with 10 mM calcium at 37 °C, before SDS−PAGE/Coomassie. (E) SPM cleavage rate for FrpA and FrpC with 10 μM of each partner, after adding 1 mM calcium for the indicated time at 25 °C. (F) Coupling rate was tested as in (E). Plots show mean ± 1 s.d., n = 3.

application of this Spy-accelerated split SPM for covalent ligation of therapeutic proteins to the unmodified Epidermal Growth Factor Receptor (EGFR) at the surface of living cells.

RESULTS

Identification of a Faster Reacting SPM Homologue. To advance NeissLock chemistry, here our first step was to explore whether other bacterial systems could give superior inducible formation of anhydrides. We bioinformatically identified a panel of SPMs with varying divergence from *N. meningitidis* FrpC (Figure S1). FrpA SPM from *N. meningitidis* shows a 98% amino acid sequence identity to FrpC SPM. SPM of the hemolysin-type calcium-binding protein-related domain-containing protein from *Alysiella filiformis* shows 71% amino acid sequence identity to FrpC. *A. filiformis* is a nonpathogenic bacterium that infects pigs.[18] SPM of the bifunctional hemolysin/adenylate cyclase precursor from *Kingella negevensis* shows 60% amino acid sequence identity to FrpC. *K. negevensis* can be found in the throat of children.[19]

As a model for NeissLock coupling, we employed the noncovalent interaction between ornithine decarboxylase (ODC) and ornithine decarboxylase antizyme (OAZ).[17] After calcium activation of NeissLock coupling, previous mass spectrometry (MS) analysis identified K92 as the primary cross-linking site on ODC, with additional cross-linking to other ε-amines proximal to the C-terminus of OAZ including K121 and K74.[17] OAZ was genetically fused to the SPM from different species. Each version was efficiently expressed solubly in *Escherichia coli*. All homologues underwent successful calcium-induced cleavage, as well as reaction to the ODC (Figure 1C). FrpA SPM was ultrafast, with 91 ± 0.2% cleaved after 1 h (Figure 1D, mean ± 1 s.d., n = 3). The few differences between SPMs of FrpA and FrpC (Figure S2A) have a major effect on the rate. We compared the time course with suboptimal conditions of temperature (25 °C) and calcium (1 mM) (Figures S2B and 1E/F). Cleavage and ligation were also substantially faster for FrpA under these conditions. Nearly 70% FrpA SPM was cleaved in 5 min, while FrpC SPM

https://doi.org/10.1021/acschembio.5c00515
ACS Chem. Biol. XXXX, XXX, XXX−XXX

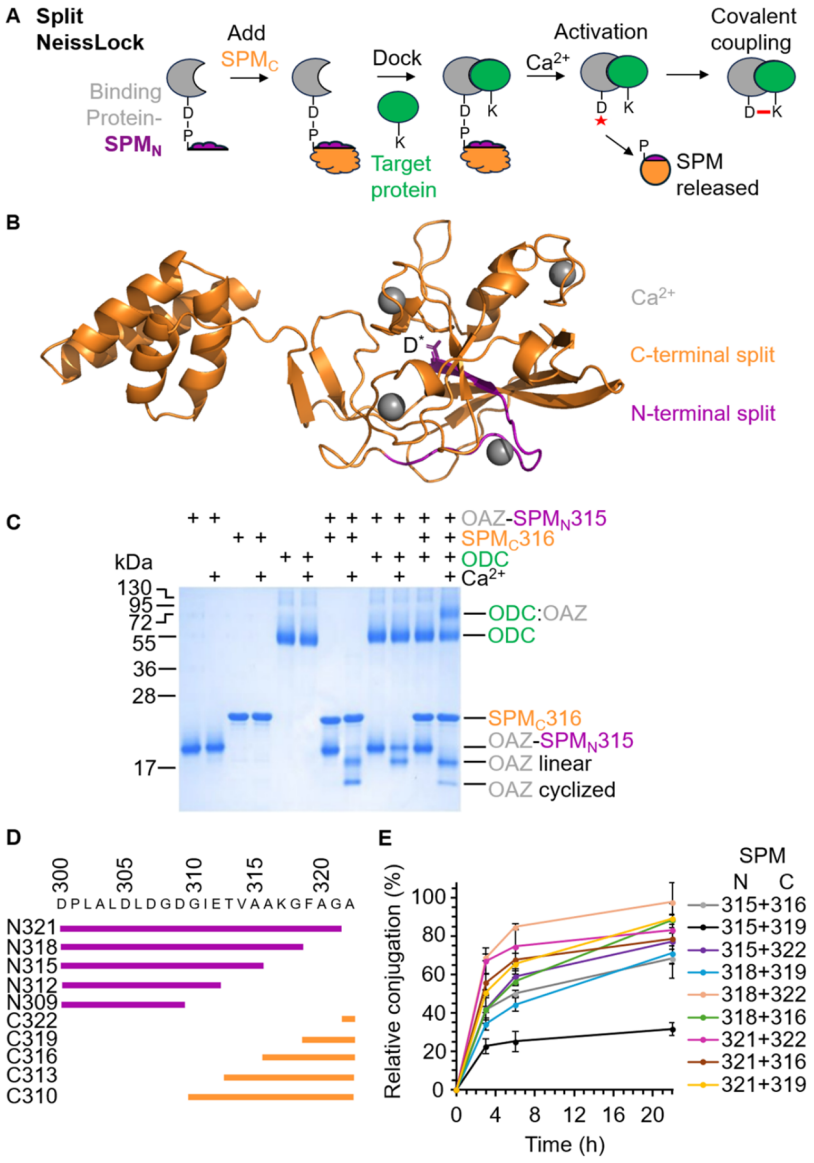

Figure 2. Engineering split NeissLock coupling. (A) Schematic of the split NeissLock. A binding protein genetically fused to the N-terminal fragment of SPM reconstitutes with SPM's C-terminal fragment, before binding the target protein. Calcium activates anhydride generation, promoting ligation to the target. (B) AlphaFold 3 model of FrpA SPM, color-coded for regions for initial splitting into N-terminal (mauve, residues 300 to 315) and C-terminal (orange, residues 316 to 543) fragments. The reactive aspartate (D*) is shown in a stick format. Ca^{2+} ions are shown as gray spheres. (C) Split NeissLock allows covalent ligation. OAZ-SPM$_N$315 and SPM$_C$316 each at 10 μM were incubated ± 10 μM ODC ± calcium at 37 °C for 16 h, before SDS−PAGE/Coomassie. (D) Schematic of the different tested SPM$_N$ and SPM$_C$ fragments. (E) Time course for ligation using SPM$_N$ and SPM$_C$ fragments. OAZ-SPM$_N$ was premixed with SPM$_C$, before incubating with ODC (each protein at 5 μM) along with calcium for the indicated times at 37 °C. Reaction was analyzed by SDS-PAGE/Coomassie (mean ± 1 s.d., n = 3).

required 60 min or longer to reach the same cleavage extent. Hence, we utilized the ultrafast FrpA SPM for subsequent engineering. Following calcium addition, the two OAZ species of differing mobility on SDS-PAGE (Figure S2B) correspond to a linear species from hydrolysis of the anhydride and a cyclized species from intramolecular reaction of the anhydride with a residue on OAZ itself, as previously validated by MS.[17] There is also potential for reaction of the anhydride with the cleaved SPM, but this side-reaction is likely to be less important since the cleaved SPM will be free to diffuse away from the OAZ-anhydride. It is unclear how frequently the SPM side-reaction with the anhydride occurs, since the product will have the same molecular weight as any OAZ-SPM that fails to be activated.

Engineering a Split SPM to Enable NeissLock Coupling with Mammalian Proteins. It is important for NeissLock to be compatible with binders expressed in the mammalian secretory pathway, since many proteins cannot be functionally expressed in bacteria because of their complex multidomain topology or obligate post-translational modification (e.g., N-linked glycosylation).[20] However, we foresaw that the millimolar calcium within the mammalian endoplasmic reticulum during secretion[21] would likely drive precleavage of SPM.[17] Indeed, when we purified superfolder green fluorescent protein (sfGFP) genetically fused to FrpA SPM, following secretion from human-derived Expi293F cells, a substantial fraction was already cleaved (Figure S3). Aiming to overcome this challenge, we devised a split protein approach, to allow

https://doi.org/10.1021/acschembio.5c00515
ACS Chem. Biol. XXXX, XXX, XXX−XXX

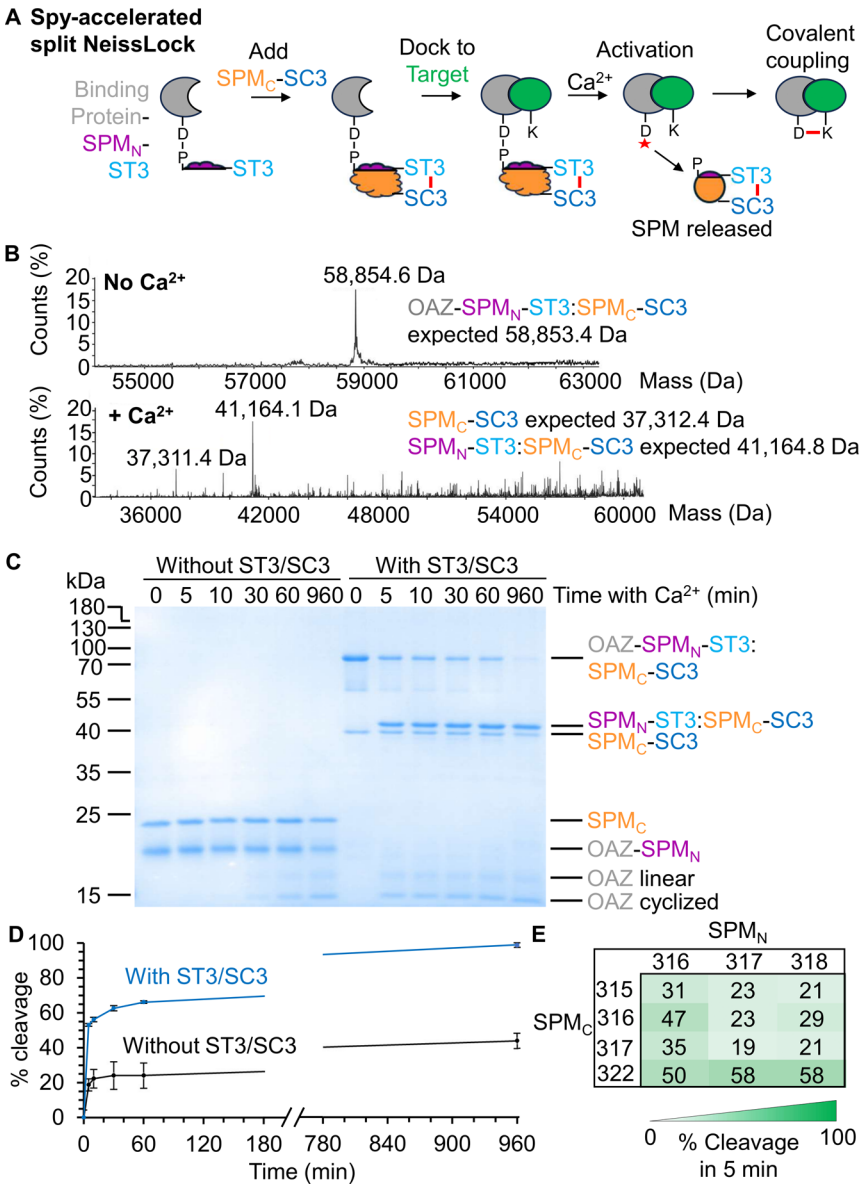

Figure 3. Spy-directed split NeissLock. (A) Schematic of Spy-accelerated split NeissLock. A binding protein fused to SPM's N-terminal fragment and SpyTag003 reacts with SPM's C-terminal fragment fused to SpyCatcher003, to promote SPM reconstitution before calcium activation. (B) Electrospray-ionization MS of reconstitution and SPM cleavage. OAZ-SPM$_N$-SpyTag003 was incubated with SPM$_C$-SpyCatcher003 and analyzed ± calcium. (C) Spy-acceleration of split SPM cleavage. 2 μM OAZ-SPM$_N$ was incubated with 2 μM SPM$_C$ ± SpyTag003/SpyCatcher003 fusion at 37 °C, before adding calcium for the indicated time and SDS-PAGE/Coomassie. (D) Quantification of Spy-accelerated cleavage, based on (C) (mean ± 1 s.d., n = 3). (E) Optimization of the Split Site for Spy-acceleration. Percentage cleavage upon mixing the OAZ-SPM$_N$-SpyTag003 and SPM$_C$-SpyCatcher003 variants was displayed as a heat map. 2 μM of each fragment was preincubated for 1 h at 37 °C, before calcium for 5 min (mean of n = 3).

efficient gating of protein function.[22,23] We designed split FrpA SPM so that NeissLock binding proteins could be expressed with a small inactive N-terminal fragment of SPM (SPM$_N$) (Figure 2A). Only upon mixing with a C-terminal fragment of SPM (SPM$_C$) should complete SPM be reconstituted, priming calcium-inducible anhydride generation. We initially split between residues 315 and 316 of FrpA SPM, to give an 18-residue N-terminal fragment, to avoid disrupting the central secondary structure (Figure 2B). The N-terminal portion comprised residues 298 to 315, with the C-terminal portion comprising the rest of the SPM. Indeed, we found calcium-induced cleavage and ligation only upon mixing the two fragments (Figure 2C).

To optimize reconstitution, we varied split positions, and constructs are named after their terminal residue (Figure 2D). Reconstitution was precarious since incubation of SPM$_N$309 with SPM$_C$310 or SPM$_N$312 with SPM$_C$313 gave no coupling (Figure S4). However, SPM$_N$318 and SPM$_C$322 gave excellent reactivity, almost twice that of the original SPM$_N$315/SPM$_C$316 (Figure 2E). The location of 318 and 322 within a loop of SPM (Figure 2B) is consistent with studies that splitting within loops is best tolerated.[22,23] Surprisingly, residues 319−321 are absent from the fastest pair. Hereafter, all experiments were performed with SPM$_N$318 (N-terminal 298−318; 21 residues) and SPM$_C$322 (C-terminal 322−543; 222 residues).

https://doi.org/10.1021/acschembio.5c00515
ACS Chem. Biol. XXXX, XXX, XXX−XXX

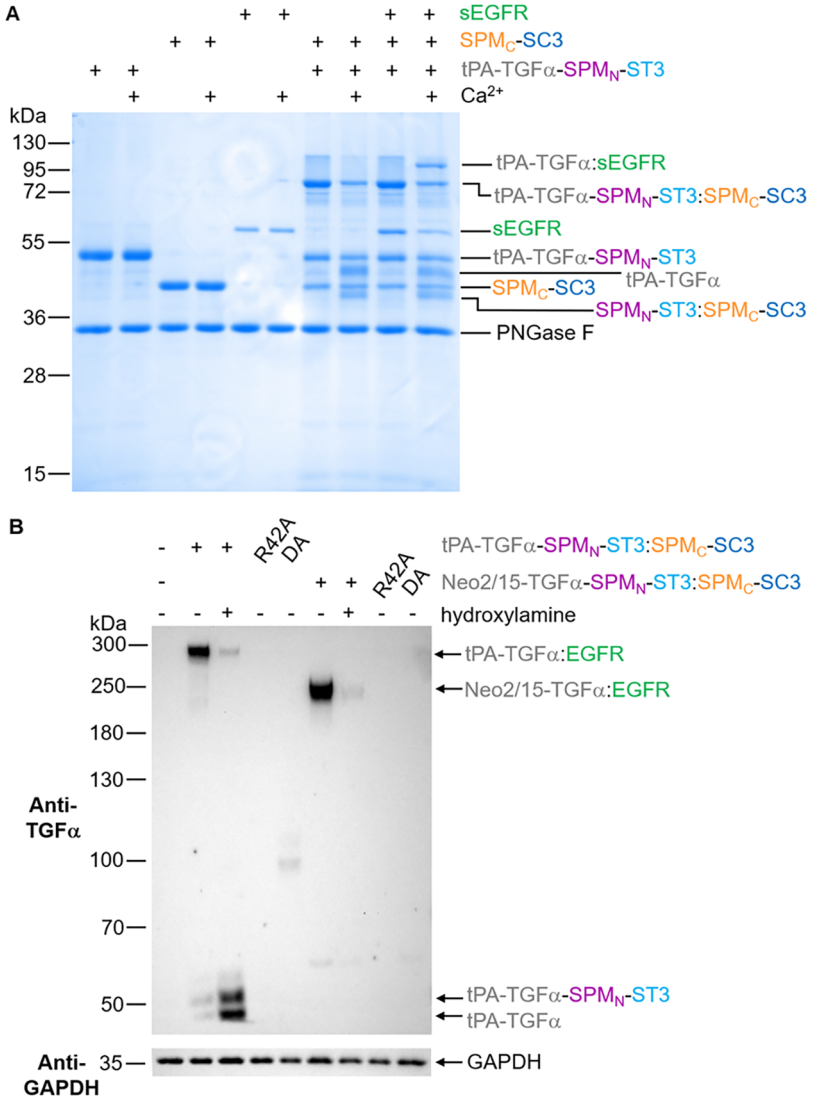

Figure 4. Spy-directed split NeissLock for coupling of model therapeutic domains to EGFR. (A) Covalent ligation of tPA to EGFR's extracellular domain. 3 μM tPA-TGFα-SPM$_N$-SpyTag003 was reconstituted with 3 μM SPM$_C$-SpyCatcher003 for 30 min at 25 °C. 1.4 μM amount of sEGFR (the soluble extracellular region of EGFR) was added for 15 min at 37 °C, followed by Ca^{2+} for 1 h at 37 °C. Coupling was analyzed by SDS-PAGE/Coomassie, after PNGase F deglycosylation to simplify banding patterns. (B) Specific coupling of tPA or cytokine domains to EGFR in living cells. A431 cells were labeled for 10 min with 2 mM calcium and 1 μM tPA or Neo2/15 linked to TGFα for split NeissLock. Covalent products were detected by Western blot with anti-TGFα. Controls have R42A TGFα to block EGFR binding, DA-mutated SPM$_N$ to block anhydride formation, or hydroxylamine to inactivate the anhydride. Blotting to GAPDH was the sample processing control.

Spy Ligation Accelerates Split FrpA Cleavage. Despite optimizing split FrpA, reactions took hours (Figure 2E) that would take minutes for full-length SPM (Figure 1F). We hypothesized that inefficient reassembly was limiting cleavage. The peptide SpyTag003 and its protein partner SpyCatcher003 react through a spontaneous isopeptide bond at rates approaching the diffusion limit,[24] thus having the potential to anchor SPM$_N$ to SPM$_C$ and facilitate reaction (Figure 3A). SpyTag003 was fused to SPM$_N$'s C-terminus, both to minimize the size of the fusion to the binding protein and to minimize the scar left in the covalent complex between the binding protein and the target (Figure 3A). SpyCatcher003 was genetically fused to SPM$_C$'s C-terminus through a short glycine/serine-containing spacer. When we modeled the structure of the complex between SPM$_N$-SpyTag003 and SPM$_C$-SpyCatcher003, AlphaFold 3 predicted the reconstitution of both the SPM$_N$/SPM$_C$ and SpyTag003/SpyCatcher003 moieties (Figure S5). We validated by MS the spontaneous isopeptide bond formation between the OAZ-SPM$_N$-SpyTag003 and SPM$_C$-SpyCatcher003 (Figure 3B).

OAZ-SPM$_N$ was mixed with SPM$_C$ with or without SpyTag003/SpyCatcher003. With Spy-assistance, 53 ± 4.3% OAZ was cleaved after 5 min and 92 ± 0.7% after 16 h (mean ± 1 s.d., n = 3). Without SpyTag003/SpyCatcher003, 19 ± 3.5% was cleaved in 5 min and only 41 ± 4.0% after 16 h (Figure 3C/D) (mean ± 1 s.d., n = 3). Hence, Spy ligation greatly accelerated split FrpA cleavage. We explored different SPM fragment lengths for further optimization of cleavage speed, but the same split sites (SPM$_N$318 and SPM$_C$322) were optimal (Figure 3E, amino acid sequences provided in Figure S6).

Split FrpA Coupling of Tissue Plasminogen Activator or Cytokine Domains to the Mammalian Cell Surface. Covalently attaching therapeutic proteins at the surface of cells

https://doi.org/10.1021/acschembio.5c00515
ACS Chem. Biol. XXXX, XXX, XXX−XXX

has the potential for improving therapeutic efficacy and pharmacokinetics. We selected the well-studied interaction between Transforming Growth Factor-α (TGFα) and EGFR for optimizing split NeissLock coupling to cells. We previously showed that NeissLock could drive covalent ligation of TGFα to EGFR on A431 cells, a human carcinoma cell line.[17] As a model therapeutic to attach, we chose tissue plasminogen activator (tPA), which cleaves plasminogen to plasmin to help degrade fibrin clots as an antithrombolytic treatment for stroke[25] and myocardial infarction.[26] Given the importance of glycosylation of tPA for activity and stability,[27] we expressed tPA-TGFα-SPM$_N$-SpyTag003 in human cells. In this construct, tPA is the model therapeutic, TGFα is the binding protein directing the interaction with EGFR, and SPM$_N$-SpyTag003 is the module for split NeissLock activation. This multimodule construct was efficiently expressed and purified by SpySwitch chromatography[28] (Figure S7), with glycosylation confirmed by Peptide N-Glycosidase F (PNGase F) digestion (Figure S8). For pilot experiments, we first tested coupling to the soluble extracellular region of EGFR (sEGFR). Previously, we showed by MS/MS that NeissLock-activated TGFα reacted with K465 of sEGFR, the closest amine to the C-terminus of TGFα.[17] We employed Spy-directed split FrpA reconstitution and added sEGFR, before activation with calcium. Using the recombinant soluble EGFR ectodomain, we observed the desired formation of the tPA-TGFα-SPM$_N$-SpyTag003:SPM$_C$-SpyCatcher003 complex, cleavage to release SPM$_N$-SpyTag003:SPM$_C$-SpyCatcher003, and formation of the tPA-TGFα:sEGFR product (Figure 4A).

We next tested coupling to endogenous EGFR at the surface of living human cells. To demonstrate the versatility of the split NeissLock approach, in addition to tPA, we also tested the coupling to cells of a second therapeutic, an interleukin-2 (IL-2) mimetic. IL-2 shows promise as a cancer therapeutic or antiviral, but life-threatening systemic toxicity has limited its use.[29] We chose to use the computationally designed Neo2/15 protein that retains high affinity for IL-2 receptor $\beta\gamma_c$ chains, but does not bind IL-2Rα or IL-15α to decrease toxicity.[29] Neo2/15 has led to enhanced therapeutic activity in models of melanoma and colon cancer compared to IL-2.[29] We genetically fused Neo2/15 to TGFα-SPM$_N$-SpyTag003, before expression in human cells and purification by SpySwitch chromatography. With split SPM, no precleavage of the Neo2/15 construct was observed during Expi293F expression (Figure S9), whereas the equivalent Neo2/15 construct with full-length SPM was almost completely cleaved by Expi293F cells (Figure S10). After reconstitution of tPA or Neo2/15 linked to TGFa-SPM$_N$-SpyTag003 with bacterially expressed SPM$_C$-SpyCatcher003 for 1 h at 25 °C, coupling of tPA or Neo2/15 to A431 cells was activated by the addition of 2 mM calcium. Cells were incubated with the proteins and calcium for 10 min at 37 °C, before subsequent washes to remove unbound proteins. Detecting by anti-TGFα Western blot, only one product band was formed on cells, consistent with the expected molecular weight of tPA or Neo2/15 fused to TGFα:EGFR, illustrating the high specificity of split NeissLock coupling (Figure 4B).

For both tPA and Neo2/15 constructs, the coupling to EGFR was almost completely abolished where hydroxylamine quenched the anhydride (Figure 4B). Hydroxylamine is a strong nucleophile that would outcompete protein nucleophiles in reacting with the cyclic anhydride.[17] This result supports the dependence of coupling on the anhydride formation. Similarly, mutating the reactive Asp in SPM to Ala (DA) blocked anhydride formation,[17] and consequently, no coupling to EGFR was observed (Figure 4B). Finally, introducing the R42A mutation to TGFα, which disrupts binding to EGFR,[30] abolished coupling to EGFR (Figure 4B). This result is consistent with the dependence on initial noncovalent EGFR binding for directing NeissLock-mediated coupling.

DISCUSSION

In summary, we have established unique characteristics of split NeissLock for covalent coupling to living cells, based on 3 advances. First, we identified how the SPM from FrpA provides an ultrafast module for anhydride formation. Second, we showed how an SPM could be dissected into a short peptide and protein partner, creating a new layer of inducibility and enabling eukaryotic expression of complex post-translationally modified building blocks for anhydride-mediated ligation. Third, we established the integration of split NeissLock with the rapid reactivity of SpyTag003/SpyCatcher003. Spy-directed split NeissLock is applicable for specific labeling under cell-compatible conditions within 10 min. Like SPM, SpyTag003/SpyCatcher003 is released from the final complex between the binding protein and the target protein following autoproteolysis. Split NeissLock avoids coupling methodologies involving ultraviolet light or free radical generation,[31] likely to cause toxicity, and avoids the complexity of noncanonical amino acid mutagenesis.[32] We demonstrated modularity by NeissLock coupling with an unmodified cellular receptor using both a therapeutic enzyme and a computationally designed cytokine. There are two regioisomers that can result from attack on a cyclic anhydride, but the regioselectivity in NeissLock is very hard to determine. Previous studies on aspartyl anhydrides showed that attack may occur at either carbonyl, with regioselectivity highly sensitive to solvent polarity and nucleophile identity.[33]

Cell therapy is delivering major impact, following clinical successes for CAR-T cells[34] and stem cells.[35] Although CAR-T cells have been approved for patients with B-cell malignancies or relapsed and/or refractory multiple myeloma, CAR-T cells have shown limited efficacy against most solid tumors, highlighting the need for strategies to enhance CAR-T cell efficacy so that more patients may benefit.[36] One such strategy is arming CAR-T cells with cytokines like IL-2 or IL-15 to enhance the potency as well as persistence of CAR-T cells.[37,38] To do so, CAR-T cells are usually genetically modified to express and secrete immunomodulatory cytokines for local delivery. However, genetic modification adds cost and prolongs the manufacturing time of CAR-T cells. Since it does not require genetic modification, we envision using split NeissLock as a fast and facile way to couple cytokines to CAR-T cells preinfusion. This could improve the CAR-T cell effector function, activate the endogenous immune system, and enhance overall immunotherapy efficacy.

Another possible application of split NeissLock is coupling therapeutic enzymes to red blood cell carriers as circulating bioreactors, capitalizing on the ~120 day circulation time of red blood cells.[39] For instance, tPA coupled to red blood cells has potential for treating patients with acute ischemic strokes.[40] Alternatively, coupling enzymes to red blood cells could help patients with orphan diseases like severe combined immunodeficiency from adenosine deaminase deficiency,[41] or Mitochondrial Neurogastrointestinal Encephalomyopathy

https://doi.org/10.1021/acschembio.5c00515
ACS Chem. Biol. XXXX, XXX, XXX−XXX

(MNGIE) from thymidine phosphorylase deficiency.[42] Currently, patients with metabolic deficiencies require regular intravenous enzyme replacement therapy infusions. By coupling enzymes to red blood cells, the frequency of the infusions could be reduced. Currently, few methods are available to modify the surface of red blood cells while preserving red blood cell function.[39,43] Split NeissLock could be used to engineer red blood cells to carry therapeutic enzymes with minimal impact on the integrity of the plasma membrane. All in all, it is vital to advance the engineering of highly reactive proteins like split NeissLock to fulfill the potential of modular cell decoration.

■ ASSOCIATED CONTENT

Supporting Information

The Supporting Information is available free of charge at https://pubs.acs.org/doi/10.1021/acschembio.5c00515.

Additional materials and methods; amino acid alignment of SPM homologs; and amino acid sequences of finalized split NeissLock pair compared to parental FrpA SPM (PDF)

■ AUTHOR INFORMATION

Corresponding Author

Mark R. Howarth − *Department of Biochemistry, University of Oxford, Oxford OX1 3QU, U.K.; Department of Pharmacology, University of Cambridge, Cambridge CB2 1PD, U.K.;* orcid.org/0000-0001-8870-7147; Email: mh2186@cam.ac.uk

Authors

Sheryl Y. T. Lim − *Department of Biochemistry, University of Oxford, Oxford OX1 3QU, U.K.;* Present Address: Institute of Molecular and Cell Biology, Agency for Science, Technology and Research (A*STAR), 61 Biopolis Drive, Singapore 138673, Singapore; orcid.org/0000-0002-2606-9220

Anthony H. Keeble − *Department of Pharmacology, University of Cambridge, Cambridge CB2 1PD, U.K.*

Complete contact information is available at: https://pubs.acs.org/10.1021/acschembio.5c00515

Author Contributions

‖S.Y.T.L. and A.H.K. contributed equally to this work.

Notes

The authors declare the following competing financial interest(s): S.Y.T.L. and M.R.H. are authors on a patent application covering sequences for anhydride formation (UK Intellectual Property Office Patent Application No. 2504781.2). S.Y.T.L. and M.R.H. are authors on a patent application covering NeissLock (UK Intellectual Property Office Patent Application No. 2003683.6). A.H.K. and M.R.H. are authors on patents covering sequences for enhanced isopeptide bond formation (UK Intellectual Property Office 1706430.4 and 1903479.2).

■ ACKNOWLEDGMENTS

S.Y.T.L. was funded by an A*STAR studentship. We thank Dr. Anthony Tumber of the University of Oxford Department of Chemistry for help with MS, through support from the Biotechnology and Biological Sciences Research Council (BBSRC, grant BB/R000344/1). A.H.K. and M.R.H. were funded by the Engineering and Physical Sciences Research Council (EPSRC EP/T030704/1).

■ REFERENCES

(1) Peschke, T.; Bitterwolf, P.; Gallus, S.; Hu, Y.; Oelschlaeger, C.; Willenbacher, N.; Rabe, K. S.; Niemeyer, C. M. Self-Assembling All-Enzyme Hydrogels for Flow Biocatalysis. *Angew. Chem., Int. Ed.* **2018**, *57*, 17028−17032.

(2) Squires, T. M.; Messinger, R. J.; Manalis, S. R. Making It Stick: Convection, Reaction and Diffusion in Surface-Based Biosensors. *Nat. Biotechnol.* **2008**, *26*, 417−426.

(3) Hills, R. A.; Howarth, M. Virus-like Particles against Infectious Disease and Cancer: Guidance for the Nano-Architect. *Curr. Opin. Biotechnol.* **2022**, *73*, 346−354.

(4) Minutolo, N. G.; Sharma, P.; Poussin, M.; Shaw, L. C.; Brown, D. P.; Hollander, E. E.; Smole, A.; Rodriguez-Garcia, A.; Hui, J. Z.; Zappala, F.; Tsourkas, A.; Powell, D. J., Jr. Quantitative Control of Gene-Engineered T-Cell Activity through the Covalent Attachment of Targeting Ligands to a Universal Immune Receptor. *J. Am. Chem. Soc.* **2020**, *142* (14), 6554−6568.

(5) Shi, Y.; Bashian, E. E.; Hou, Y.; Wu, P. Chemical Immunology: Recent Advances in Tool Development and Applications. *Cell Chem. Biol.* **2024**, *31* (3), 387−408.

(6) Spanedda, M. V.; Bourel-Bonnet, L. Cyclic Anhydrides as Powerful Tools for Bioconjugation and Smart Delivery. *Bioconjugate Chem.* **2021**, *32* (3), 482−496.

(7) Wang, Z.; Liu, P. K.; Li, L. A Tutorial Review of Labeling Methods in Mass Spectrometry-Based Quantitative Proteomics. *ACS Meas. Sci. Au.* **2024**, *4* (4), 315−337.

(8) Holm, L.; Moody, P.; Howarth, M. Electrophilic Affibodies Forming Covalent Bonds to Protein Targets. *J. Biol. Chem.* **2009**, *284*, 32906−32913.

(9) Chmura, A. J.; Orton, M. S.; Meares, C. F. Antibodies with Infinite Affinity. *Proc. Natl. Acad. Sci. U.S.A.* **2001**, *98*, 8480−8484.

(10) Qiu, J.; Nie, Y.; Zhao, Y.; Zhang, Y.; Li, L.; Wang, R.; Wang, M.; Chen, S.; Wang, J.; Li, Y.-Q.; Xia, J. Safeguarding Intestine Cells against Enteropathogenic *Escherichia Coli* by Intracellular Protein Reaction, a Preventive Antibacterial Mechanism. *Proc. Natl. Acad. Sci. U.S.A.* **2020**, *117* (10), 5260−5268.

(11) Liu, J.; Yang, B.; Wang, L. Residue Selective Crosslinking of Proteins through Photoactivatable or Proximity-Enabled Reactivity. *Curr. Opin. Chem. Biol.* **2023**, *74*, No. 102285.

(12) Zhang, H.; Han, Y.; Yang, Y.; Lin, F.; Li, K.; Kong, L.; Liu, H.; Dang, Y.; Lin, J.; Chen, P. R. Covalently Engineered Nanobody Chimeras for Targeted Membrane Protein Degradation. *J. Am. Chem. Soc.* **2021**, *143* (40), 16377−16382.

(13) Xuan, W.; Li, J.; Luo, X.; Schultz, P. G. Genetic Incorporation of a Reactive Isothiocyanate Group into Proteins. *Angew. Chem., Int. Ed.* **2016**, *55* (34), 10065−10068.

(14) Wang, N.; Yang, B.; Fu, C.; Zhu, H.; Zheng, F.; Kobayashi, T.; Liu, J.; Li, S.; Ma, C.; Wang, P. G.; Wang, Q.; Wang, L. Genetically Encoding Fluorosulfate-l-tyrosine To React with Lysine, Histidine, and Tyrosine via SuFEx in Proteins in Vivo. *J. Am. Chem. Soc.* **2018**, *140* (15), 4995−4999.

(15) Osicka, R.; Prochazkova, K.; Sulc, M.; Linhartova, I.; Havlicek, V.; Sebo, P. A Novel "Clip-and-Link" Activity of Repeat in Toxin (RTX) Proteins from Gram-Negative Pathogens. *J. Biol. Chem.* **2004**, *279*, 24944−24956.

(16) Sadilkova, L.; Osicka, R.; Sulc, M.; Linhartova, I.; Novak, P.; Sebo, P. Single-Step Affinity Purification of Recombinant Proteins Using a Self-Excising Module from Neisseria Meningitidis FrpC. *Protein Sci.* **2008**, *17*, 1834−1843.

(17) Scheu, A. H. A.; Lim, S. Y. T.; Metzner, F. J.; Mohammed, S.; Howarth, M. NeissLock Provides an Inducible Protein Anhydride for Covalent Targeting of Endogenous Proteins. *Nat. Commun.* **2021**, *12*, No. 717.

(18) Zutic, J.; Radosavljevic, V.; Radanovic, O.; Ivetic, V.; Pavlovic, I.; Zutic, M. A Case Report: Isolation of Alysiella Filiformis from Pig's Lungs. *Kafkas Univ. Vet. Fak. Derg.* **2013**, *19* (4), 721−723.

(19) Yagupsky, P.; El Houmami, N.; Fournier, P.-E. Respiratory Carriage of the Novel Kingella Negevensis Species by Young Children. *New Microbes New Infect.* **2018**, *26*, 59−62.
(20) Schütz, A.; Bernhard, F.; Berrow, N.; Buyel, J. F.; Ferreira-da-Silva, F.; Haustraete, J.; van den Heuvel, J.; Hoffmann, J.-E.; de Marco, A.; Peleg, Y.; Suppmann, S.; Unger, T.; Vanhoucke, M.; Witt, S.; Remans, K. A Concise Guide to Choosing Suitable Gene Expression Systems for Recombinant Protein Production. *STAR Protocols* **2023**, *4* (4), No. 102572.
(21) Mekahli, D.; Bultynck, G.; Parys, J. B.; De Smedt, H.; Missiaen, L. Endoplasmic-Reticulum Calcium Depletion and Disease. *Cold Spring Harbor Perspect. Biol.* **2011**, *3* (6), No. a004317.
(22) Dagliyan, O.; Krokhotin, A.; Ozkan-Dagliyan, I.; Deiters, A.; Der, C. J.; Hahn, K. M.; Dokholyan, N. V. Computational Design of Chemogenetic and Optogenetic Split Proteins. *Nat. Commun.* **2018**, *9* (1), No. 4042.
(23) Anastassov, S.; Filo, M.; Khammash, M. Inteins: A Swiss Army Knife for Synthetic Biology. *Biotechnol. Adv.* **2024**, *73*, No. 108349.
(24) Keeble, A. H.; Turkki, P.; Stokes, S.; Anuar, I. N. A. K.; Rahikainen, R.; Hytonen, V. P.; Howarth, M. Approaching Infinite Affinity through Engineering of Peptide-Protein Interaction. *Proc. Natl. Acad. Sci. U.S.A.* **2019**, *116*, 26523−26533.
(25) Zhu, A.; Rajendram, P.; Tseng, E.; Coutts, S. B.; Yu, A. Y. X. Alteplase or Tenecteplase for Thrombolysis in Ischemic Stroke: An Illustrated Review. *Res. Pract. Thromb. Haemostasis* **2022**, *6* (6), No. e12795.
(26) Guillermin, A.; Yan, D. J.; Perrier, A.; Marti, C. Safety and Efficacy of Tenecteplase versus Alteplase in Acute Coronary Syndrome: A Systematic Review and Meta-Analysis of Randomized Trials. *Arch. Med. Sci.* **2016**, *6*, 1181−1187.
(27) Toul, M.; Slonkova, V.; Mican, J.; Urminsky, A.; Tomkova, M.; Sedlak, E.; Bednar, D.; Damborsky, J.; Hernychova, L.; Prokop, Z. Identification, Characterization, and Engineering of Glycosylation in Thrombolytics. *Biotechnol. Adv.* **2023**, *66*, No. 108174.
(28) Vester, S. K.; Rahikainen, R.; Khairil Anuar, I. N. A.; Hills, R. A.; Tan, T. K.; Howarth, M. SpySwitch Enables pH- or Heat-Responsive Capture and Release for Plug-and-Display Nanoassembly. *Nat. Commun.* **2022**, *13* (1), No. 3714.
(29) Silva, D.-A.; Yu, S.; Ulge, U. Y.; Spangler, J. B.; Jude, K. M.; Labão-Almeida, C.; Ali, L. R.; Quijano-Rubio, A.; Ruterbusch, M.; Leung, I.; Biary, T.; Crowley, S. J.; Marcos, E.; Walkey, C. D.; Weitzner, B. D.; Pardo-Avila, F.; Castellanos, J.; Carter, L.; Stewart, L.; Riddell, S. R.; Pepper, M.; Bernardes, G. J. L.; Dougan, M.; Garcia, K. C.; Baker, D. De Novo Design of Potent and Selective Mimics of IL-2 and IL-15. *Nature* **2019**, *565* (7738), 186−191.
(30) Lazar, E.; Vicenzi, E.; Van Obberghen-Schilling, E.; Wolff, B.; Dalton, S.; Watanabe, S.; Sporn, M. B. Transforming Growth Factor Alpha: An Aromatic Side Chain at Position 38 Is Essential for Biological Activity. *Mol. Cell. Biol.* **1989**, *9* (2), 860−864.
(31) Gentzel, M.; Pardo, M.; Subramaniam, S.; Stewart, A. F.; Choudhary, J. S. Proteomic Navigation Using Proximity-Labeling. *Methods* **2019**, *164−165*, 67−72.
(32) de la Torre, D.; Chin, J. W. Reprogramming the Genetic Code. *Nat. Rev. Genet.* **2021**, *22* (3), 169−184.
(33) Huang, X.; Luo, X.; Roupioz, Y.; Keillor, J. W. Controlled Regioselective Anilide Formation from Aspartic and Glutamic Acid Anhydrides. *J. Org. Chem.* **1997**, *62* (25), 8821−8825.
(34) Qin, V. M.; D'Souza, C.; Neeson, P. J.; Zhu, J. J. Chimeric Antigen Receptor beyond CAR-T Cells. *Cancers* **2021**, *13* (3), No. 404.
(35) Blanc, K. L.; Dazzi, F.; English, K.; Farge, D.; Galipeau, J.; Horwitz, E. M.; Kadri, N.; Krampera, M.; Lalu, M. M.; Nolta, J.; Patel, N. M.; Shi, Y.; Weiss, D. J.; Viswanathan, S. ISCT MSC Committee Statement on the US FDA Approval of Allogenic Bone-Marrow Mesenchymal Stromal Cells. *Cytotherapy* **2025**, *27*, 413−416.
(36) Du, B.; Qin, J.; Lin, B.; Zhang, J.; Li, D.; Liu, M. CAR-T Therapy in Solid Tumors. *Cancer Cell* **2025**, *43* (4), 665−679.
(37) Tang, L.; Pan, S.; Wei, X.; Xu, X.; Wei, Q. Arming CAR-T Cells with Cytokines and More: Innovations in the Fourth-Generation CAR-T Development. *Mol. Ther.* **2023**, *31* (11), 3146−3162.
(38) Liu, Y.; Adu-Berchie, K.; Brockman, J. M.; Pezone, M.; Zhang, D. K. Y.; Zhou, J.; Pyrdol, J. W.; Wang, H.; Wucherpfennig, K. W.; Mooney, D. J. Cytokine Conjugation to Enhance T Cell Therapy. *Proc. Natl. Acad. Sci. U.S.A.* **2023**, *120* (1), No. e2213222120.
(39) Brenner, J. S.; Mitragotri, S.; Muzykantov, V. R. Red Blood Cell Hitchhiking: A Novel Approach for Vascular Delivery of Nanocarriers. *Annu. Rev. Biomed. Eng.* **2021**, *23*, 225−248.
(40) Armstead, W. M.; Ganguly, K.; Riley, J.; Zaitsev, S.; Cines, D. B.; Higazi, A. A.; Muzykantov, V. R. RBC-Coupled tPA Prevents Whereas tPA Aggravates JNK MAPK-Mediated Impairment of ATP- and Ca-Sensitive K Channel-Mediated Cerebrovasodilation After Cerebral Photothrombosis. *Transl. Stroke Res.* **2012**, *3*, 114−121.
(41) Secord, E.; Hartog, N. L. Review of Treatment for Adenosine Deaminase Deficiency (ADA) Severe Combined Immunodeficiency (SCID). *Ther. Clin. Risk Manage.* **2022**, *18*, 939−944.
(42) Levene, M.; Bain, M. D.; Moran, N. F.; Nirmalananthan, N.; Poulton, J.; Scarpelli, M.; Filosto, M.; Mandel, H.; MacKinnon, A. D.; Fairbanks, L.; Pacitti, D.; Bax, B. E. Safety and Efficacy of Erythrocyte Encapsulated Thymidine Phosphorylase in Mitochondrial Neurogastrointestinal Encephalomyopathy. *J. Clin. Med.* **2019**, *8* (4), No. 457.
(43) Shi, J.; Kundrat, L.; Pishesha, N.; Bilate, A.; Theile, C.; Maruyama, T.; Dougan, S. K.; Ploegh, H. L.; Lodish, H. F. Engineered Red Blood Cells as Carriers for Systemic Delivery of a Wide Array of Functional Probes. *Proc. Natl. Acad. Sci. U.S.A.* **2014**, *111*, 10131−10136.

https://doi.org/10.1021/acschembio.5c00515
ACS Chem. Biol. XXXX, XXX, XXX−XXX

Supporting information for:

Split NeissLock with Spy-acceleration arms mammalian proteins for anhydride-mediated cell ligation

Sheryl Y.T. Lim[1,2*], Anthony H. Keeble[3*] and Mark R. Howarth[1,3†]

[1]Department of Biochemistry, University of Oxford, South Parks Road, Oxford OX1 3QU, U.K.
[2]Current address: Institute of Molecular and Cell Biology, Agency for Science, Technology and Research (A*STAR), 61 Biopolis Drive, Singapore 138673, Singapore
[3]Department of Pharmacology, University of Cambridge, Tennis Court Road, Cambridge CB2 1PD, U.K.
* S.Y.T.L. and A.H.K. contributed equally to this work

†Corresponding author and Lead Contact:
Mark R. Howarth,
Department of Pharmacology,
University of Cambridge,
Tennis Court Road,
Cambridge,
CB2 1PD,
U.K.
E-mail: mh2186@cam.ac.uk

Materials and Methods

Bacterial strains

E. coli NEB Turbo cells (New England Biolabs) were used to amplify plasmids and were grown in LB medium with antibiotic at 37 °C. Proteins were expressed in *E. coli* BL21(DE3) RIPL (Agilent).

Cell-lines

Mammalian proteins were expressed in Expi293F cells (Thermo Fisher), maintained in Expi293 Expression media (Thermo Fisher) supplemented with 50 U/mL penicillin/streptomycin (Thermo Fisher). Cells were grown in a humidified Multitron Cell incubator (Infors HT) at 37 °C with 7% (v/v) CO_2, rotating at 110 to 125 rpm. A431 cells, a human epidermoid carcinoma cell-line from Cancer Research UK, Lincoln's Inn Fields, were grown in complete media [Dulbecco's Modified Eagle Medium–high glucose (DMEM) supplemented with 10% (v/v) fetal bovine serum (FBS), penicillin/streptomycin (Gibco, 100 U/mL), and 1× GlutaMAX (Gibco)] at 37 °C, with 5% (v/v) CO_2.

Plasmids and cloning

Plasmids were constructed using PCR-based cloning methods with Q5 High-Fidelity 2× master mix (New England Biolabs) or KOD polymerase (EMD Millipore), followed by Gibson assembly. Synthetic gene fragments were either codon-optimized for expression in *E. coli* and ordered from Integrated DNA Technologies before cloning into the pET28a backbone for bacterial expression, or codon-optimized for expression in mammalian cells before cloning into pcDNA3.1 or pENTR4 backbones for mammalian expression. The open-reading frames of all constructs were validated by Sanger sequencing (Source Bioscience).

Human ornithine decarboxylase 1 (ODC) was cloned as pET28a-His_6-ODC-Ctag (GenBank MW364944, Addgene plasmid #163614) and previously described[1]. Residues 95-219 of human OAZ (UniProt P54368) with sequence numbering based on OAZ/ODC crystal structure (PDB 4ZGY)[2] was used. Residue numbers for the FrpC self-processing module (SPM) span amino acid residues 414–657 of FrpC from *N. meningitidis* serogroup B (strain MC58) (UniProt Q9JYV5)[3]. This FrpC SPM was cloned as pET28a-AviTag-His_6-OAZ-GSY-SPM-Ctag with a mutation (C175A) in OAZ to minimize disulfide-based aggregation[1]. This construct formed the basis for the cloning of alternative SPM domains. pET28a-AviTag-His_6-OAZ-SPM(FrpA)-Ctag (GenBank PX255652, Addgene plasmid #246646) was cloned using the FrpA SPM based on position 298-543 of FrpA from *Neisseria meningitidis* serotype C (UniProt P55126). pET28a-AviTag-His_6-OAZ-SPM(*A. filiformis*)-Ctag (GenBank PX255653) was cloned using the SPM based on residues 231-476 of hemolysin-type calcium-binding protein related domain-containing protein from *Alysiella filiformis* (GenBank: SOD68839.1). pET28a-AviTag-His_6-OAZ-SPM(*K. negevensis*)-Ctag (GenBank PX255654) was cloned using the SPM based on residues 190-434 of the bifunctional hemolysin/adenylate cyclase precursor from *Kingella negevensis* (GenBank: SNB83338.1). The native -1 and -2 residues relative to the cleavable Asp-Pro bond were retained in these constructs to promote efficient activity[1]. Split FrpA SPM N-terminal variants were cloned from pET28a-AviTag-His_6-OAZ-SPM(FrpA)-Ctag with differing lengths to the SPM (C-terminal deletions) and with the C-tag deleted. Constructs pET28a-AviTag-His_6-OAZ-SPM(FrpA 298-315), pET28a-AviTag-His_6-OAZ-SPM(FrpA 298-318), and pET28a-AviTag-His_6-OAZ-SPM(FrpA 298-321) were cloned in a similar manner, with the numbers referring to the residues of the N-terminal part of the SPM retained in the construct. Constructs pET28a-AviTag-His_6-OAZ-SPM(FrpA 298-316)-GSG-SpyTag003, pET28a-AviTag-His_6-OAZ-SPM(FrpA 298-317)-GSG-SpyTag003 and pET28a-AviTag-His_6-OAZ-SPM(FrpA 298-318)-GSG-SpyTag003 (GenBank PX255655,

Addgene plasmid # 246647) contain an extra GSG spacer followed by a SpyTag003 at the C-terminus. C-terminal variants were cloned from pET28a-AviTag-His_6-OAZ-SPM(FrpA)-Ctag with differing lengths to the SPM (N-terminal deletions) and retained C-tag. Constructs pET28a-SPM(FrpA 315-543)-Ctag, pET28a-SPM(FrpA 316-543)-Ctag, pET28a-SPM(FrpA 317-543)-Ctag, pET28a-SPM(FrpA 319-543)-Ctag, and pET28a-SPM(FrpA 322-543)-Ctag were cloned with the numbers referring to the residues of the C-terminal part of the SPM retained in the construct. Variants with SpyCatcher003 domains following the C-terminal variants were cloned from these plasmids with the arrangement SPM(FrpA C-term portion)-GSGAM linker-SpyCatcher003-GSSGSGSG-Ctag. Constructs pET28a-SPM(FrpA 315-543)-SpyCatcher003-Ctag, pET28a-SPM(FrpA 316-543)-SpyCatcher003-Ctag, pET28a-SPM(FrpA 317-543)-SpyCatcher003-Ctag, and pET28a-SPM(FrpA 322-543)-SpyCatcher003-Ctag were cloned in this manner. pET28a-His_6-SUMO-SPM_C-SpyCatcher003-Ctag (GenBank PX255656, Addgene plasmid # 246648) was cloned from pET28a-SPM(FrpA 322-543)-SpyCatcher003-Ctag. pENTR4-sEGFR-His_6, encoding a soluble fragment of the extracellular domain of human EGFR (UniProt P00533, residues 25–525), has been described[1]. pOPINE His_6- SUMO protease Ulp1 has been described[4]. pcDNA3.1 AP-His_6-sfGFP-SPM was cloned with the domain organization: tPA signal peptide, AviTag biotinylation peptide-His_6-sfGFP-FrpA full-length SPM. pcDNA3.1 tPA-TGFα-SPM_N-SpyTag003 (GenBank PX255657, Addgene plasmid # 246649) was cloned with the organization: tPA signal peptide, Kringle domain of human tPA, protease domain of human tPA containing the mutations found in Tenectaplase (K296A, H297A, R298A and R299A) that result in enhanced resistance to the plasma inhibitor PAI-1[5], GSS linker, TGFα (residues 40–89 of human protransforming growth factor alpha), SPM(FrpA 298-318), GSG linker, SpyTag003. pcDNA3.1 tPA-TGFα (R42A)-SPM_N-SpyTag003 was cloned from pcDNA3.1 tPA-TGFα-SPM_N-SpyTag003 with mutation of Arg42 of the TGFα sequence to alanine[6]. pcDNA3.1 tPA-TGFα-SPM_N DA-SpyTag003 was cloned from pcDNA3.1 tPA-TGFα-SPM_N-SpyTag003 with mutation at the aspartic acid residue that forms the anhydride. pcDNA3.1 Neo2/15-TGFα-SPM_N-SpyTag003 (GenBank PX255658, Addgene plasmid # 246650) was cloned with the following organization: tPA signal peptide, Neo2/15[7], GSS linker, TGFα (residues 40–89 of human protransforming growth factor alpha), GSY, SPM(FrpA 298-318), GSG linker, SpyTag003. pcDNA3.1 Neo2/15-TGFα (R42A)-SPM_N-SpyTag003 was cloned from pcDNA3.1 Neo2/15-TGFα-SPM_N-SpyTag003 with mutation of Arg42 of the TGFα sequence to alanine[6]. pcDNA3.1 Neo2/15-TGFα-SPM_N DA-SpyTag003 was cloned from pcDNA3.1 Neo2/15-TGFα-SPM_N-SpyTag003 with mutation at the aspartic acid residue that forms the anhydride. pcDNA3.1 Neo2/15-TGFα-SPM-His_6 was cloned from pcDNA3.1 Neo2/15-TGFα-SPM_N-SpyTag003 by cloning FrpA SPM-His_6 in place of SPM_N-SpyTag003.

Bacterial protein expression and purification

Bacterial expression was in *E. coli* BL21(DE3) RIPL cells. After transformation of the plasmids into the growth strain, the cells were recovered on LB agar plates + 50 μg/mL kanamycin overnight at 37 °C. Single colonies were picked into starter cultures of 10 mL LB containing 25 μg/mL kanamycin and grown for 16 h at 37 °C with shaking at 200 rpm. Expression cultures were inoculated with 1/100 dilution of the saturated starter in 1 L LB + 0.8% (w/v) glucose [for expressions in BL21(DE3) RIPL] supplemented with 25 μg/mL kanamycin in ultra-yield baffled flasks (Thomson Instrument Company). Cultures were grown at 37 °C with shaking at 200 rpm until A_{600} 0.5 and protein expression was induced with 0.42 mM isopropyl β-D-1-thiogalactopyranoside (IPTG) with shaking at 200 rpm at 25 °C for 18 h. Cells were harvested by centrifugation and processed immediately or stored at -80 °C.

For proteins without His_6-tags but containing C-tags, cells were resuspended in ice-cold bacterial lysis buffer [30 mM Tris-HCl pH 7.4, 200 mM NaCl, 5% (v/v) glycerol, cOmplete

mini EDTA-free protease inhibitor cocktail, 1 mM phenylmethylsulfonyl fluoride (PMSF), 1 mg/mL lysozyme (Merck) and 2 U/mL benzonase (Merck)]. Cells were lysed by sonication on ice, with the cells sonicated 3–4 times for 1 min at 50% duty cycle with 1 min rest periods. Cell lysate was clarified for 30 min by centrifugation in a JA25−50 rotor (Beckman) at 30,000–35,000 g at 4 °C. The clarified lysate was incubated with CaptureSelect C-tagXL Affinity Matrix (Thermo Fisher) resin pre-equilibrated with C-tag binding/wash buffer (30 mM Tris-HCl pH 7.4, 200 mM NaCl) in a Poly-Prep gravity column and mixed by rotation for 30-60 min at 4 °C. The column was drained, the resin washed with binding/wash buffer, and proteins eluted in 50 mM HEPES plus 2 M $MgCl_2$, pH 7.4, with all washes and elution steps at 4 °C. Protein concentrations were determined from A_{280} using the extinction coefficient from ExPASy ProtParam. Typical yields were 8-15 mg/L culture.

For proteins purified by His_6-tag, cells were resuspended in ice-cold bacterial lysis buffer supplemented with 10 mM imidazole, pH 7.4. Cells were lysed by sonication on ice, with the cells sonicated 3–4 times for 1 min at 50% duty cycle with 1 min rest periods. Cell lysate was clarified for 45 min by centrifugation in a JA25−50 rotor (Beckman) at 30,000–35,000 g at 4 °C. The clarified lysate was incubated with Ni-NTA resin (Qiagen) pre-equilibrated with Ni-NTA binding/wash buffer (30 mM Tris-HCl, 200 mM NaCl, 10 mM imidazole pH 7.4) in a Poly-Prep gravity column and mixed by rotation for 30-60 min at 4 °C. The column was drained and the resin was washed with binding/wash buffer, before eluting in 30 mM Tris-HCl pH 7.4, 200 mM NaCl, plus 200 mM imidazole at 4 °C. When purifying ODC or OAZ variants, 5 mM 2-mercaptoethanol was supplemented in wash and elution buffers. Typical yields were 8-15 mg/L culture.

After either His_6-tag or C-tag purification, eluted proteins were concentrated using a Vivaspin centrifugal concentrator with 10 or 30 kDa cut-off (GE Healthcare) and centrifuged at 4,000 g at 4 °C. A HiLoad 16/600 Superdex 200 pg column (GE Healthcare) was connected to the ÄKTA pure 25 fast protein liquid chromatography (FPLC) system (GE Healthcare) for size-exclusion chromatography (SEC). The column was pre-equilibrated with running buffer [50 mM HEPES pH 7.4, 150 mM NaCl, 2 mM tris(2-carboxyethyl)phosphine (TCEP)] for gel filtration of OAZ and ODC. When purifying ODC variants, the running buffer was supplemented with an additional 0.02 mM pyridoxal phosphate (Sigma-Aldrich) as co-factor. Proteins samples were loaded at 1 mL/min and isocratic elution was carried out with 1 mL fractions collected. Based on the A_{280} peak, fractions of interest were collected and the purity of the fractions was verified by SDS-PAGE/Coomassie. Fractions containing the protein of interest were concentrated to ~500 µL using a Vivaspin centrifugal concentrator with 10 or 30 kDa cut-off (GE Healthcare). Long-term storage of the proteins was at -80 °C.

For SUMO domain removal, His_6-SUMO-SPM_C-SpyCatcher003-Ctag was dialyzed into TBS pH 7.5 (50 mM Tris-HCl pH 7.5, 150 mM NaCl) and concentrated using a Vivaspin centrifugal concentrator with a 10 kDa cut-off (GE Healthcare). SUMO protease Ulp1[4] was added at 1:50 molar ratio, followed by 45 min incubation at 25 °C. Remaining His_6-tagged proteins (SUMO and Ulp1) in a volume of 800 µL were incubated with 200 µL Ni-NTA (Qiagen) with rotation for 1 h on a tube rotor at 25 °C, followed by application to a Polyprep column and collection of the column flow-through containing the SPM_C-SpyCatcher003-Ctag.

Mammalian protein expression and purification

Neo2/15-TGFα-SPM_N-SpyTag003 variants, tPA-TGFα-SPM_N-SpyTag003 variants, and sEGFR-His_6 were expressed by transient transfection in Expi293F cells (Thermo Fisher). Cells were grown in a humidified Multitron Cell incubator (Infors HT) at 37 °C with 8% (v/v) CO_2, rotating at 95 rpm to 3.0×10^6 cells/mL in Expi293 expression media supplemented with 50 U/mL penicillin/streptomycin (Thermo Fisher). Cells were transferred into Expi293 expression media with no antibiotics present and transfected with plasmid using the ExpiFectamine 293

Transfection Kit (Thermo Fisher). Plasmid DNA (1 μg per mL of culture) was incubated with ExpiFectamine 293 reagent for 20 min and then added dropwise to the Expi293F cells. Cells were grown for 20 h before addition of ExpiFectamine 293 Transfection Enhancers 1 and 2. When expressing sEGFR, kifunensine (Sigma-Aldrich) was added to the culture concurrent to transfection to a final 5 μM to promote homogeneous glycosylation. Proteins were harvested 4-8 days post-transfection.

Proteins containing a His_6-tag were purified by Ni-NTA (Qiagen). The cell supernatant was harvested and then we added $1/10^{th}$ volume of 10× Ni-NTA binding buffer, mixed protease inhibitors (cOmplete mini EDTA-free protease inhibitor cocktail, Roche) and imidazole to a final 10 mM. Resin was pre-equilibrated with Ni-NTA binding/wash buffer (30 mM Tris-HCl, 200 mM NaCl, 10 mM imidazole, pH 7.4) and incubated with the cell supernatant in a Poly-Prep gravity column and mixed by rotation for 30-60 min at 4 °C. The column was drained, the resin was washed with Ni-NTA binding/wash buffer, and proteins were eluted in 30 mM Tris-HCl, 200 mM NaCl, 200 mM imidazole, pH 7.4 at 4 °C.

Proteins containing SpyTag003 but no His_6-tag were purified by SpySwitch[8]. The cell supernatant was harvested and $1/10^{th}$ volume of 10× SpySwitch buffer (500 mM Tris-HCl pH 7.5 + 3 M NaCl) was added, supplemented with mixed protease inhibitors (cOmplete mini EDTA-free protease inhibitor cocktail, Roche). Resin was pre-equilibrated with SpySwitch binding buffer (50 mM Tris-HCl pH 7.5, 300 mM NaCl) and incubated with the cell supernatant in a Poly-Prep gravity column, with mixing by rotation for 30-60 min at 4 °C. The column was drained and the resin was washed with SpySwitch buffer at 4 °C. Proteins were eluted with 1.5 column volumes of SpySwitch elution buffer (50 mM acetic acid/sodium acetate pH 5.0, 150 mM NaCl) at 4 °C and the elution was collected into a microcentrifuge tube containing 0.3 column volumes of 1 M Tris-HCl pH 8.0, with the microcentrifuge tube mixed by inversion to minimize time spent at an acidic pH. Typical yields of proteins were 4-8 mg/L culture.

Polyacrylamide gel electrophoresis

SDS-PAGE was performed using 7-14% polyacrylamide gels in an XCell SureLock system (Thermo Scientific). Electrophoresis was carried out at 180-200 V in 25 mM Tris-HCl pH 8.5, 192 mM glycine, 0.1% (w/v) SDS. For 7% Tris-Acetate gels, electrophoresis was carried at 180 V in 50 mM Tricine, 50 mM Tris base, pH 8.24, 0.1% (w/v) SDS. Gels were stained with Brilliant Blue G-250 and destained with Milli-Q H_2O, prior to imaging on a ChemiDoc XRS+ imager. ImageLab 6.1.0 software (Bio-Rad) was used for densitometric quantification. For imaging on an iBright FL1500 imaging system (Thermo Fisher), analysis was performed using iBright Analysis Software Versions 5.0.1 and 5.2.0 (Thermo Fisher). On gels, a colon between proteins indicates conjugates that are hypothesized to be covalently coupled.

SPM cleavage and protein conjugation assays

Reactions were carried out at 37 °C (except when otherwise stated) in HEPES-buffered saline (HBS: 50 mM HEPES pH 7.4, 150 mM NaCl), supplemented with 2 mM TCEP when ODC proteins were included. Cleavage of SPM was initiated by addition of pre-warmed reaction buffer containing calcium chloride to the required concentration. Reactions were incubated for the desired time and quenched by addition of EDTA, to chelate Ca^{2+}, in 5× SDS-loading buffer [0.19 M Tris-HCl pH 6.8, 20% (v/v) glycerol, 100 μM bromophenol blue, 0.19 M SDS] with EDTA at 15 mM and heating at 95 °C for 5 min in a C1000 Touch Thermal Cycler (Bio-Rad). The degree of SPM cleavage and coupling was assessed by SDS-PAGE/Coomassie densitometry. Assays were run in triplicate and the percentage cleavage/coupling expressed as the mean ± 1 S.D. from n=3.

Cleavage and coupling reactions of ODC with SPM homologs were carried out with 5 μM ODC pre-mixed with 5 μM OAZ-SPM variants in HBS + 2 mM TCEP at 37 °C. Reaction

was activated by addition of a final concentration of 10 mM $CaCl_2$. Reaction aliquots were sampled across a range of time-points.

Detailed comparison of the cleavage and coupling reactions between ODC and FrpC or FrpA SPMs was repeated with modified conditions. 10 μM ODC was pre-mixed with either OAZ-SPM(FrpC) or OAZ-SPM(FrpA) in HBS + 2 mM TCEP at 25 °C and reaction was activated by addition of a final concentration of 1 mM $CaCl_2$. Reaction aliquots were sampled across a range of time-points.

Initial comparison of the split FrpA calcium-induced cleavage and coupling to ODC was carried out with 10 μM of OAZ-SPM-N terminal variant incubated with 10 μM of SPM-C terminal variant with or without 10 μM ODC and 10 mM Ca^{2+} in HBS + 2 mM TCEP, at 37 °C for 16 h. Time-courses for the conjugation to ODC with different split variants were repeated with activation by 10 mM Ca^{2+} in HBS + 2 mM TCEP at 37 °C, but with 5 μM OAZ-SPM_N terminal variant incubated with 5 μM SPM_C terminal variant and 5 μM ODC before Ca^{2+} activation. Reaction aliquots were sampled across a range of time-points.

For comparison of the impact of proximity labeling with SpyTag003/SpyCatcher003 on Ca^{2+}-induced cleavage of the optimized split FrpA SPM, the two half-proteins were mixed and incubated in HBS at 37 °C for 1 h. In parallel experiments 2 μM OAZ-SPM_N318 was incubated with 2 μM SPM_C322, whilst 2 μM OAZ-SPM_N318-SpyTag003 was incubated with 2 μM SPM_C322-SpyCatcher003. 10 mM Ca^{2+} was then added to initiate cleavage and reaction aliquots were sampled across a range of time-points.

For coupling of SPM-reconstituted Neo2/15-TGFα-SPM_N-SpyTag003 and tPA-TGFα-SPM_N-SpyTag003 with sEGFR, reactions were carried out in HBS. In parallel reactions, 3 μM SPM_C-SpyCatcher003-Ctag was incubated with 3 μM Neo2/15-TGFα-SPM_N-SpyTag003 and tPA-TGFα-SPM_N-SpyTag003 for 30 min at 37 °C. 1.54 μM sEGFR was then added and equilibrated for 30 min at 37 °C, before activation with a final 2 mM Ca^{2+} for 1 h. Control reactions without Ca^{2+} or sEGFR were also carried out. Post-reaction samples were digested with Peptide:N-glycosidase F (PNGase F) under denaturing conditions. Glycoprotein Denaturing Buffer (10× stock, NEB) was added to a final concentration of 1×, and samples were heated for 10 min at 100 °C. After cooling to 25 °C, Glycoprotein Buffer 2 (NEB) was added to 1×, NP-10 (NEB) was added to 10% (v/v), and PNGase F (NEB) was added to 50,000 U/mL. Samples were then digested for 1 h at 37 °C before SDS-PAGE.

Calculation of SPM cleavage and coupling

The percentage SPM cleaved was calculated using Equation 1.

$$\%\ Cleavage = \left(1 - \left(\frac{Intensity\ of\ SPM\ band\ at\ time\ t}{Intensity\ of\ SPM\ band\ at\ time\ 0}\right)\right) \times 100 \qquad \text{Equation 1}$$

The percentage of ODC coupled was calculated using Equation 2.

$$\%\ ODC\ coupled = \left(1 - \left(\frac{Intensity\ of\ ODC\ band\ at\ time\ t}{Intensity\ of\ ODC\ band\ at\ time\ 0}\right)\right) \times 100 \qquad \text{Equation 2}$$

The relative conjugation between ODC and OAZ was calculated in Equation 3 as the band intensity of the OAZ:ODC conjugate divided by the band intensity of OAZ:ODC at 22 h for the most efficient reaction for the different versions of the split FrpA reacted together.

$$Relative\ \%\ conjugated = \left(\frac{OAZ{:}ODC\ at\ time\ t}{Max\ OAZ{:}ODC\ at\ 22h}\right) \times 100$$

Equation 3

Coupling of SPM proteins to EGFR on live cells

A431 cells were seeded in a 6-well plate at 5×10^5 cells/well and incubated at 37 °C with 5% (v/v) CO_2 in complete growth media for 24 h. Cells were then washed twice with 4 mL washes

of FBS-free complete media. A431 cells were grown serum-starved for a further 24 h at 37 °C with 5% (v/v) CO_2. Cells were then washed twice with 2 mL HBS-Mg (50 mM HEPES pH 7.4, 150 mM NaCl, 5 mM $MgCl_2$, sterile-filtered). In parallel reactions, 150 µL 2 µM Neo2/15-TGFα-SPM_N-SpyTag003 and tPA-TGFα-SPM_N-SpyTag003 were each reconstituted with 2 µM SPM_C-SpyCatcher003-Ctag for 1 h at 25 °C in HBS-Mg. These were then added to a well, with or without hydroxylamine (Sigma-Aldrich) dissolved to a final 5 mM in 2% (v/v) dimethylsulfoxide (DMSO) in HBS-Mg. Coupling was activated by the rapid subsequent addition of 150 µL 4 mM $CaCl_2$ in HBS-Mg, with or without hydroxylamine dissolved to final 5 mM. The cells were incubated with the SPM-containing proteins and 2 mM $CaCl_2$ for 10 min at 37 °C with 5% (v/v) CO_2, before removal of the protein solution. The cells were then incubated in FBS-free complete media containing 2% (v/v) DMSO, with or without 5 mM hydroxylamine for 1 h. After removal of the media, A431 cells were lysed by addition of 150 µL ice-cold modified RIPA buffer [20 mM Tris-HCl pH 7.4, 150 mM NaCl, 5 mM NaF, 1% (v/v) Triton-X-100, 0.1% (w/v) SDS, 0.5% (w/v) sodium deoxycholate], supplemented with cOmplete protease inhibitor mix, 1 mM PMSF and 1 mM sodium orthovanadate and scraping of the cells from the plate, followed by incubation for 20 min at 4 °C. The cell lysate was pipetted from the plates and the cleared lysate was produced by centrifugation at 12,000 g for 20 min at 4 °C.

Western blotting

Aliquots of cleared lysates were mixed with 6× SDS loading buffer containing 10 mM dithiothreitol and heated at 95 °C for 5 min in a C1000 Touch Thermal Cycler (Bio-Rad), before running on 7% Tris-Acetate SDS-PAGE for detection of TGFα-containing bands. After electrophoresis, gels were incubated in 20% (v/v) ethanol for 20 min. Proteins were transferred at 15 V for 13 min when using the iBlot 2 Dry Blotting System (Thermo Fisher). The membrane was incubated in blocking solution of 5 % (w/v) milk (Sigma-Aldrich) in TBS-T [50 mM Tris-HCl pH 7.4, 150 mM NaCl, 0.1% (v/v) Tween 20] for 1 h at 25 °C. When blotting for TGFα, the anti-TGFα antibody (MF9, Novus Biologicals) was added at 1:1,000 in the blocking solution and the membrane was incubated for 20 h at 4 °C. The membranes were then washed 4 × 5 min in TBS-T, before addition of the secondary antibody. Goat anti-mouse horseradish peroxidase (HRP) (A4416, Merck) was diluted to 1:1,000 in the blocking solution and the membranes were incubated with the antibody for 1 h at 25 °C, before another 4 × 5 min washes in TBS-T. Proteins were detected using SuperSignal West Pico PLUS Chemiluminescent Substrate (Thermo Fisher), measuring chemiluminescence on an iBright FL1500 imaging system (Thermo Fisher) with analysis using iBright Analysis Software Versions 5.0.1 and 5.2.0 (Thermo Fisher).

When detecting glyceraldehyde-3-phosphate dehydrogenase (GAPDH) as a sample processing control, aliquots of cleared lysates were mixed with 6× SDS loading buffer containing 10 mM dithiothreitol and heated at 95 °C for 5 min in a C1000 Touch Thermal Cycler (Bio-Rad) before running on a 14% Tris-glycine SDS-PAGE. After electrophoresis, transfer of bands to the membrane and blocking in TBS-T + 5 % (w/v) milk was performed as described above. GAPDH was detected using 1:1,000 mouse anti-GAPDH GA1R (Thermo Fisher) (20 h at 4 °C) and 1:2,000 Goat-anti-mouse-HRP (A4416, Merck) (1 h at 25 °C) both in 5% (w/v) skimmed milk in TBS-T. Proteins were detected as described above.

Mass Spectrometry

Purified protein constructs were analyzed with a jet-stream electrospray ionization intact protein mass spectrometry experiment, using a RapidFire 365 jet-stream electrospray ion source (Agilent) coupled to a 6550 Accurate-Mass Quadrupole Time-of-Flight (Q-TOF) (Agilent) mass spectrometer in positive ion mode. 10 µM protein samples were injected and

acidified to 0.9 % (v/v) formic acid. Samples were aspirated for 0.3 s before they were adsorbed onto a C4 solid-phase cartridge for extraction. Washes using 0.1% (v/v) formic acid were carried out for 5.5 s before elution onto the detector for 5.5 s. Data were analyzed using Mass Hunter Qualitative Analysis software B.07.00 (Agilent). Protein ionization was deconvoluted using the maximum entropy algorithm. Expected molecular weights for full-length proteins were calculated using ExPASy ProtParam, with the N-terminal fMet (bacterial expression) removed. For constructs where a SpyTag003 and SpyCatcher003 reacted with one another, isopeptide bond formation occurs releasing a water molecule, which was taken into account when calculating the expected molecular weight.

Graphics and structure analysis

Structures were visualized in PyMOL version 2.0.6 (DeLano Scientific), with FrpA split sites guided by the nuclear magnetic resonance structure of the Ca^{2+}-bound FrpC SPM (PDB 6SJW)[9]. The sequence alignment of the SPM variants was created using Clustal Omega. The model structure of the Ca^{2+}-bound FrpA SPM, comprising residues 298-543 of FrpA from *N. meningitidis* serotype C (UniProt P55126), was generated using AlphaFold 3[10] with the expected 4 Ca^{2+} ions selected to be included in the model. The model of the SPM_N-ST3:SPM_C-SC3 complex was generated using AlphaFold 3[10] using the finalized sequences for the constructs in Figure S6. The expected 4 Ca^{2+} ions were also included in the model.

Statistics and reproducibility

No statistical method was used to pre-determine sample sizes. No data were excluded from our analyses. Experiments were not randomized. The investigators were not blinded to allocation during the experiments and assessment of outcome.

Data availability

Sequences of key constructs are found in GenBank, as described in the section “Plasmids and cloning”. Plasmids from this study have been deposited in the Addgene repository (https://www.addgene.org/Mark_Howarth/), as described in the section “Plasmids and cloning”. Further information and request for resources and reagents should be directed to and will be fulfilled by the lead contact, M.R.H.

REFERENCES

(1) Scheu, A. H. A.; Lim, S. Y. T.; Metzner, F. J.; Mohammed, S.; Howarth, M. NeissLock Provides an Inducible Protein Anhydride for Covalent Targeting of Endogenous Proteins. *Nat. Commun*. **2021**, *12*, 717. https://doi.org/10.1038/s41467-021-20963-5.

(2) Wu, H.-Y.; Chen, S.-F.; Hsieh, J.-Y.; Chou, F.; Wang, Y.-H.; Lin, W.-T.; Lee, P.-Y.; Yu, Y.-J.; Lin, L.-Y.; Lin, T.-S.; Lin, C.-L.; Liu, G.-Y.; Tzeng, S.-R.; Hung, H.-C.; Chan, N.-L. Structural Basis of Antizyme-Mediated Regulation of Polyamine Homeostasis. *Proc. Natl. Acad. Sci. U.S.A.* **2015**, *112* (36), 11229–11234. https://doi.org/10.1073/pnas.1508187112.

(3) Osicka, R.; Prochazkova, K.; Sulc, M.; Linhartova, I.; Havlicek, V.; Sebo, P. A Novel “Clip-and-Link” Activity of Repeat in Toxin (RTX) Proteins from Gram-Negative Pathogens. Covalent Protein Cross-Linking by an Asp-Lys Isopeptide Bond upon Calcium-Dependent Processing at an Asp-Pro Bond. *J. Biol. Chem.* **2004**, *279*, 24944–24956. https://doi.org/10.1074/jbc.M314013200.

(4) Assenberg, R.; Delmas, O.; Graham, S. C.; Verma, A.; Berrow, N.; Stuart, D. I.; Owens, R. J.; Bourhy, H.; Grimes, J. M. Expression, Purification and Crystallization of a

Lyssavirus Matrix (M) Protein. *Acta Crystallogr. Sect. F Struct. Biol. Cryst. Commun.* **2008**, *64*, 258–262. https://doi.org/10.1107/S1744309108004557.
(5) Zhu, A.; Rajendram, P.; Tseng, E.; Coutts, S. B.; Yu, A. Y. X. Alteplase or Tenecteplase for Thrombolysis in Ischemic Stroke: An Illustrated Review. *Res. Pract. Thromb. Haemost.* **2022**, *6* (6), e12795. https://doi.org/10.1002/rth2.12795.
(6) Lazar, E.; Vicenzi, E.; Van Obberghen-Schilling, E.; Wolff, B.; Dalton, S.; Watanabe, S.; Sporn, M. B. Transforming Growth Factor Alpha: An Aromatic Side Chain at Position 38 Is Essential for Biological Activity. *Mol. Cell. Biol.* **1989**, *9* (2), 860–864. https://doi.org/10.1128/mcb.9.2.860-864.1989.
(7) Silva, D.-A.; Yu, S.; Ulge, U. Y.; Spangler, J. B.; Jude, K. M.; Labão-Almeida, C.; Ali, L. R.; Quijano-Rubio, A.; Ruterbusch, M.; Leung, I.; Biary, T.; Crowley, S. J.; Marcos, E.; Walkey, C. D.; Weitzner, B. D.; Pardo-Avila, F.; Castellanos, J.; Carter, L.; Stewart, L.; Riddell, S. R.; Pepper, M.; Bernardes, G. J. L.; Dougan, M.; Garcia, K. C.; Baker, D. De Novo Design of Potent and Selective Mimics of IL-2 and IL-15. *Nature* **2019**, *565* (7738), 186–191. https://doi.org/10.1038/s41586-018-0830-7.
(8) Vester, S. K.; Rahikainen, R.; Khairil Anuar, I. N. A.; Hills, R. A.; Tan, T. K.; Howarth, M. SpySwitch Enables pH- or Heat-Responsive Capture and Release for Plug-and-Display Nanoassembly. *Nat. Commun.* **2022**, *13* (1), 3714. https://doi.org/10.1038/s41467-022-31193-8.
(9) Kuban, V.; Macek, P.; Hritz, J.; Nechvatalova, K.; Nedbalcova, K.; Faldyna, M.; Sebo, P.; Zidek, L.; Bumba, L. Structural Basis of Ca2+-Dependent Self-Processing Activity of Repeat-in-Toxin Proteins. *mBio* **2020**, *11* (2), e00226-20. https://doi.org/10.1128/mBio.00226-20.
(10) Abramson, J.; Adler, J.; Dunger, J.; Evans, R.; Green, T.; Pritzel, A.; Ronneberger, O.; Willmore, L.; Ballard, A. J.; Bambrick, J.; Bodenstein, S. W.; Evans, D. A.; Hung, C.-C.; O'Neill, M.; Reiman, D.; Tunyasuvunakool, K.; Wu, Z.; Žemgulytė, A.; Arvaniti, E.; Beattie, C.; Bertolli, O.; Bridgland, A.; Cherepanov, A.; Congreve, M.; Cowen-Rivers, A. I.; Cowie, A.; Figurnov, M.; Fuchs, F. B.; Gladman, H.; Jain, R.; Khan, Y. A.; Low, C. M. R.; Perlin, K.; Potapenko, A.; Savy, P.; Singh, S.; Stecula, A.; Thillaisundaram, A.; Tong, C.; Yakneen, S.; Zhong, E. D.; Zielinski, M.; Žídek, A.; Bapst, V.; Kohli, P.; Jaderberg, M.; Hassabis, D.; Jumper, J. M. Accurate Structure Prediction of Biomolecular Interactions with AlphaFold 3. *Nature* **2024**, *630* (8016), 493–500. https://doi.org/10.1038/s41586-024-07487-w.

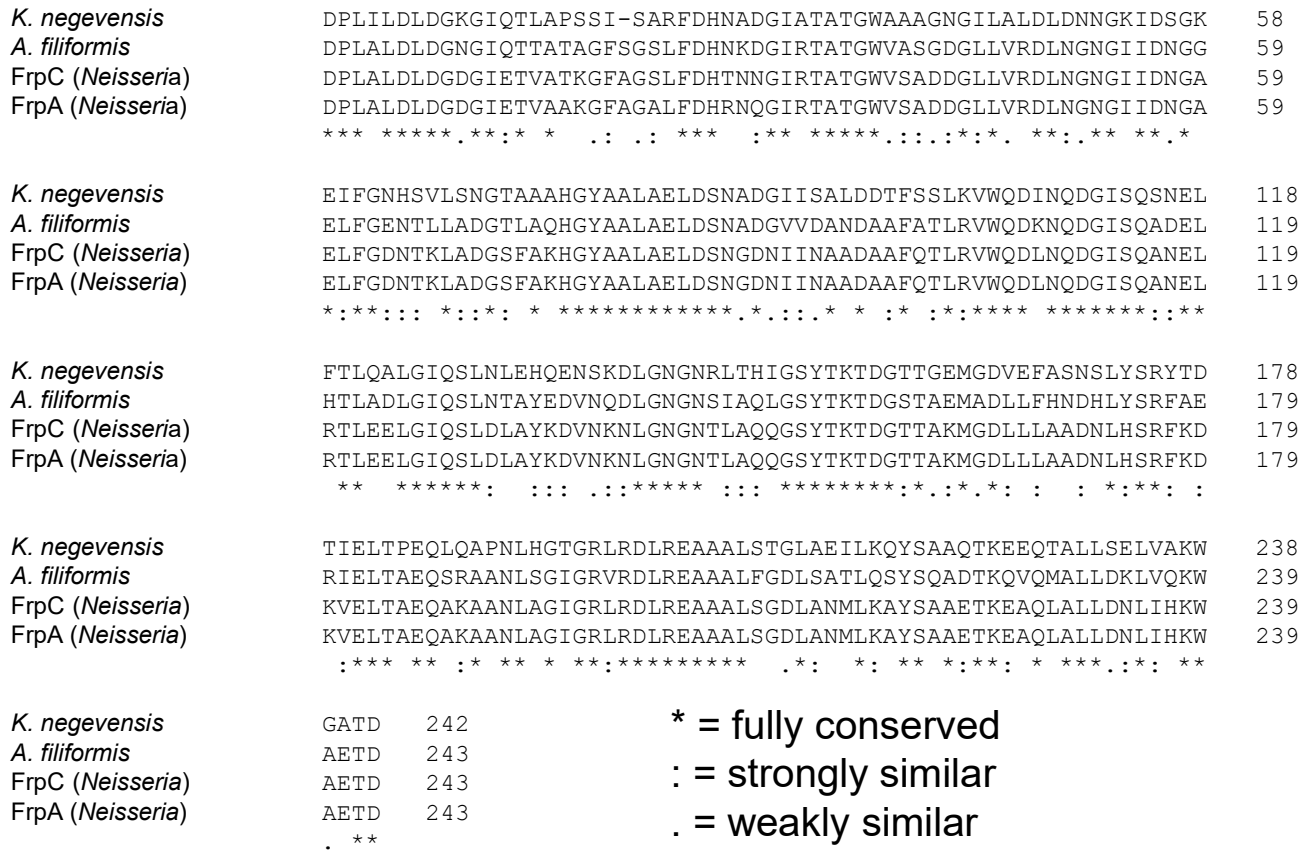

Figure S1: Amino acid alignment of SPM homologs. *Kingella negevensis* SPM is based on the bifunctional hemolysin/adenylate cyclase precursor. *Alysiella filiformis* SPM is based on the hemolysin-type calcium-binding protein related domain-containing protein. FrpC SPM is shown from *N. meningitidis* serogroup B (strain MC58). FrpA SPM is from *N. meningitidis* serotype C.

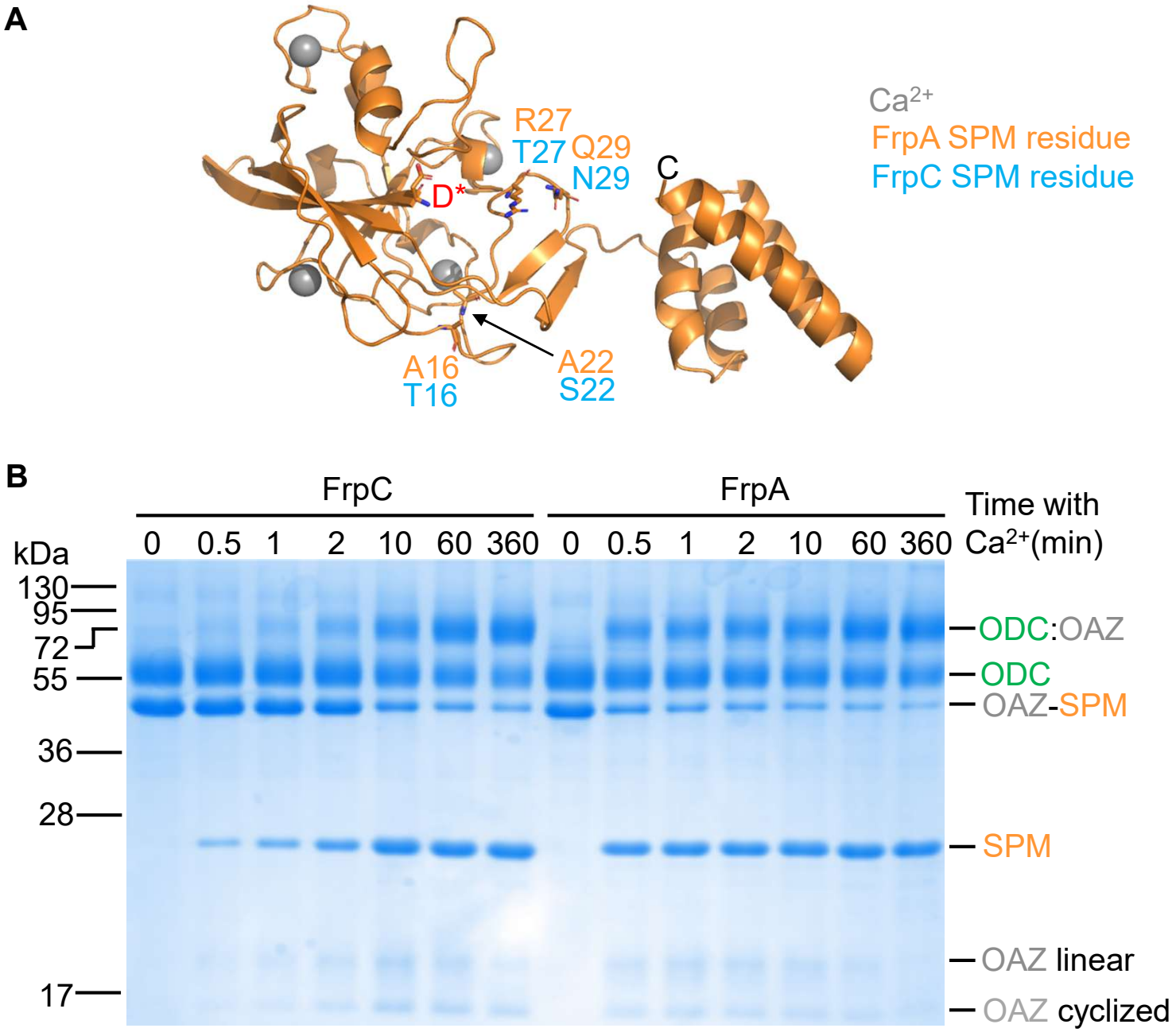

Figure S2: FrpA has faster protein-protein ligation than FrpC. (A) AlphaFold 3 model of FrpA SPM, with calcium as gray spheres. The FrpA residues where there are sequence differences in FrpC are shown in stick format. D* shows the aspartate in stick format where reaction occurs. **(B)** Reaction of 10 μM ODC with OAZ-SPM for FrpC (left) or FrpA (right) for varying times at 25 °C, analyzed by SDS-PAGE/Coomassie.

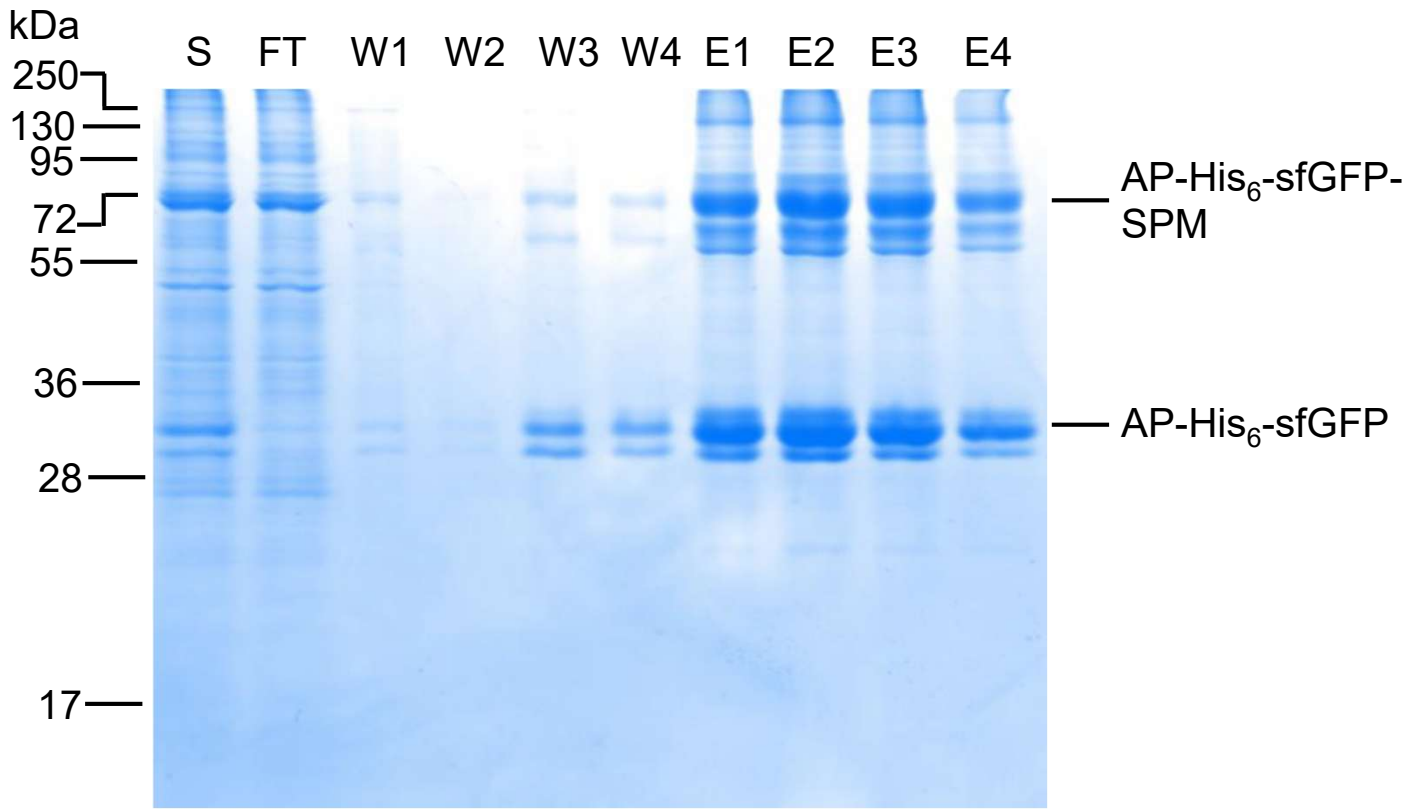

Figure S3: Premature cleavage of AP-His_6-sfGFP-SPM after purification from mammalian cells. AP-His_6-sfGFP-SPM, targeted for secretion, was purified from the supernatant of Expi293F cells by Ni-NTA after transient transfection. Fractions are analyzed by SDS-PAGE under reducing conditions with Coomassie staining. S supernatant; FT flow-through; W1-W4 column washes; E1-E4 elution fractions. The band corresponding to the molecular weight of full-length AP-His_6-sfGFP-SPM is marked, as well as the band corresponding to AP-His_6-sfGFP where SPM has been cleaved.

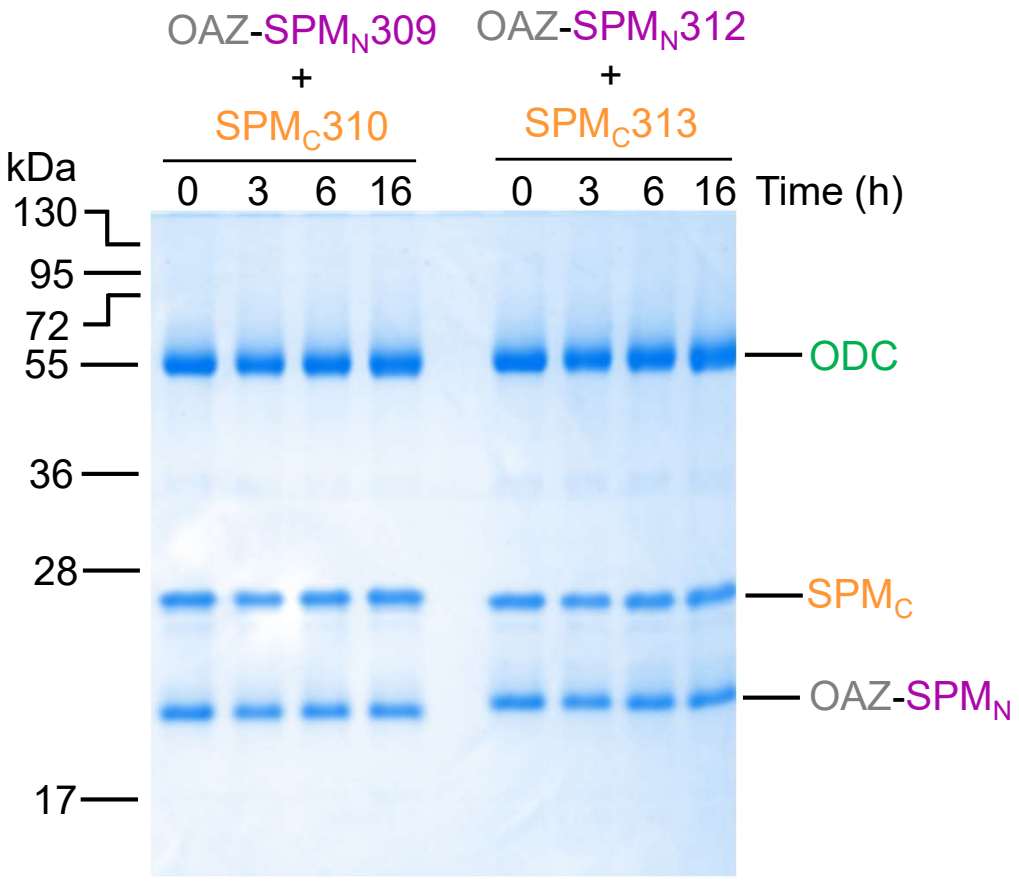

Figure S4: Example N-terminal (OAZ-SPM_N) and C-terminal (SPM_C) split FrpA constructs that do not reconstitute for reaction. Different 5 μM N-terminal (OAZ-SPM_N) and 5 μM C-terminal (SPM_C) split FrpA constructs were incubated with 5 μM ODC and activated with 10 mM Ca^{2+} for the indicated time at 37 °C. No product formation was observed even after 16 h reaction, based on SDS-PAGE with Coomassie staining.

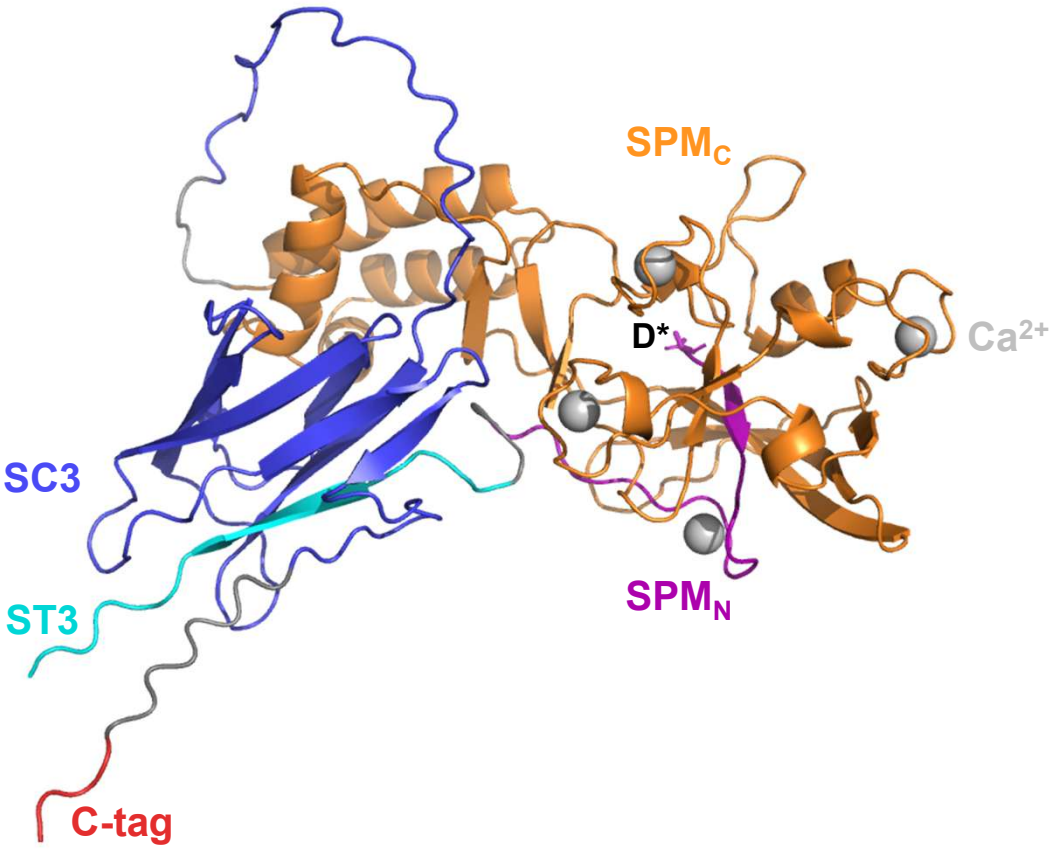

Figure S5: AlphaFold 3 model of the reconstituted SPM$_N$-ST3:SPM$_C$-SC3 complex. This model shows the form with calcium ions bound, representing the state before reaction at the aspartate (D*), whose side-chain is shown in stick format. SPM$_N$ in purple; ST3 in cyan; SC3 in dark blue; SPM$_C$ in orange; linkers in gray; C-tag in red; Ca^{2+} as a gray sphere.

Full-length FrpA SPM

```
   300         310         320         330         340         350
VYDPLALDLDGDGIETVAAKGFAGALFDHRNQGIRTATGWVSADDGLLVRDLNGNGIIDNG
  360         370         380         390         400         410
AELFGDNTKLADGSFAKHGYAALAELDSNGDNIINAADAAFQTLRVWQDLNQDGISQANEL
420         430         440         450         460         470         480
RTLEELGIQSLDLAYKDVNKNLGNGNTLAQQGSYTKTDGTTAKMGDLLLAADNLHSRFKDK
            490         500         510         520         530         540
VELTAEQAKAANLAGIGRLRDLREAAALSGDLANMLKAYSAAETKEAQLALLDNLIHKWAE

TD
```

SPM_N-SpyTag003

```
   300         310
SYDPLALDLDGDGIETVAAKGGSGRGVPHIVMVDAYKRYK
```

SPM_C-SpyCatcher003-Ctag

```
          330         340         350         360         370         380
ALFDHRNQGIRTATGWVSADDGLLVRDLNGNGIIDNGAELFGDNTKLADGSFAKHGYAALA
        390         400         410         420         430         440
ELDSNGDNIINAADAAFQTLRVWQDLNQDGISQANELRTLEELGIQSLDLAYKDVNKNLGN
      450         460         470         480         490         500
GNTLAQQGSYTKTDGTTAKMGDLLLAADNLHSRFKDKVELTAEQAKAANLAGIGRLRDLRE
    510         520         530         540
AAALSGDLANMLKAYSAAETKEAQLALLDNLIHKWAETDGSGAMVTTLSGLSGEQGPSGDM

TTEEDSATHIKFSKRDEDGRELAGATMELRDSSGKTISTWISDGHVKDFYLYPGKYTFVET

AAPDGYEVATPIEFTVNEDGQVTVDGEATEGDAHTGSSGSGSGEPEA
```

Figure S6: Amino acid sequences of finalized split NeissLock pair compared to parental FrpA SPM. Residue numbers are based on the full-length SPM. SPM_N in purple; ST3 in cyan; SC3 in dark blue; SPM_C in orange; linkers in black; C-tag in red.

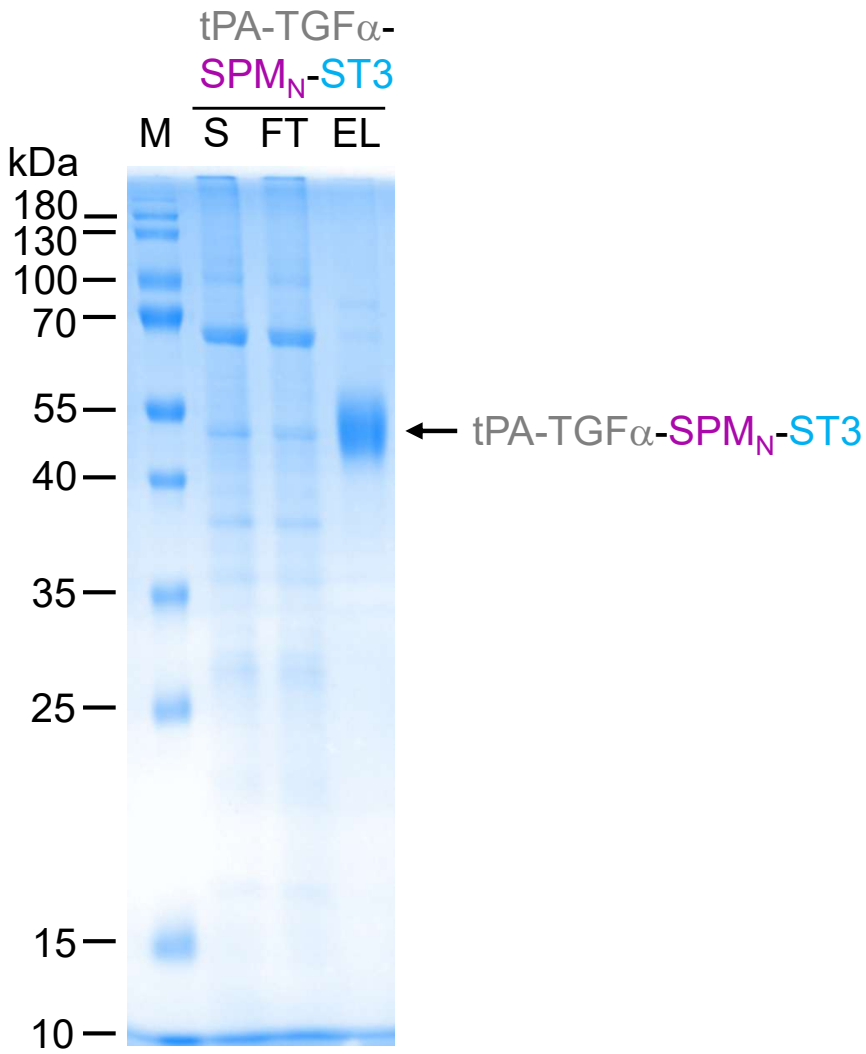

Figure S7: Effective purification of tPA-TGFα-SPM$_N$-ST3 after secretion from mammalian cells. tPA-TGFα-SPM$_N$-ST3 was purified from the supernatant of Expi293F cells by SpySwitch affinity purification after transient transfection. Fractions were reduced with DTT and analyzed by SDS-PAGE with Coomassie staining. M marker; S supernatant; FT flow-through; EL concentrated elution fractions.

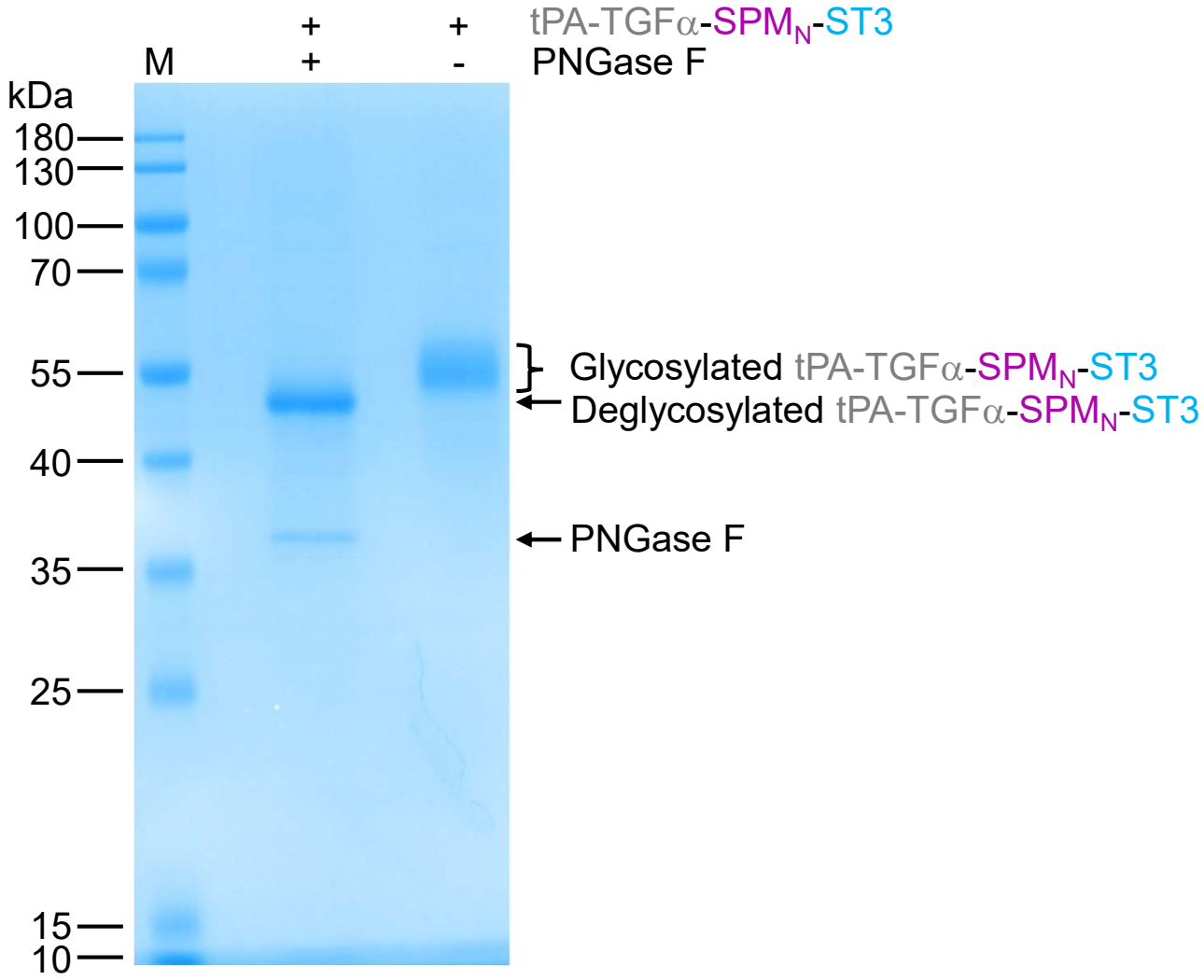

Figure S8: tPA-TGFα-SPM$_N$-ST3 is glycosylated when expressed using Expi293F cells. Purified tPA-TGFα-SPM$_N$-ST3 with or without PNGase F digestion was analyzed by SDS-PAGE with Coomassie staining. M is the molecular weight marker.

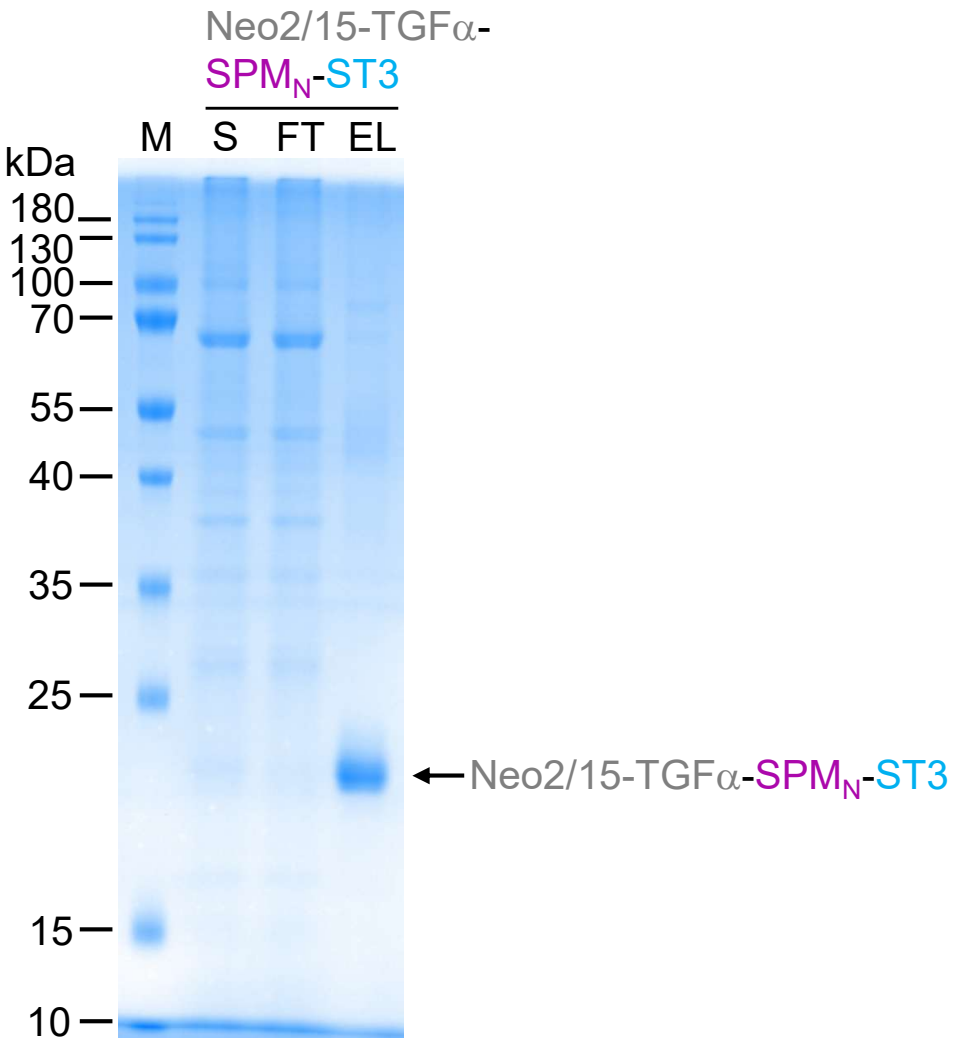

Figure S9: Effective purification of Neo2/15-TGFα-SPM$_N$-ST3 after secretion from mammalian cells. Neo2/15-TGFα-SPM$_N$-ST3 was purified from the supernatant of Expi293F cells by SpySwitch affinity purification after transient transfection. Fractions were reduced with DTT and analyzed by SDS-PAGE with Coomassie staining. M = marker, S = Cell supernatant, FT = column flow-through, EL = concentrated elution fractions

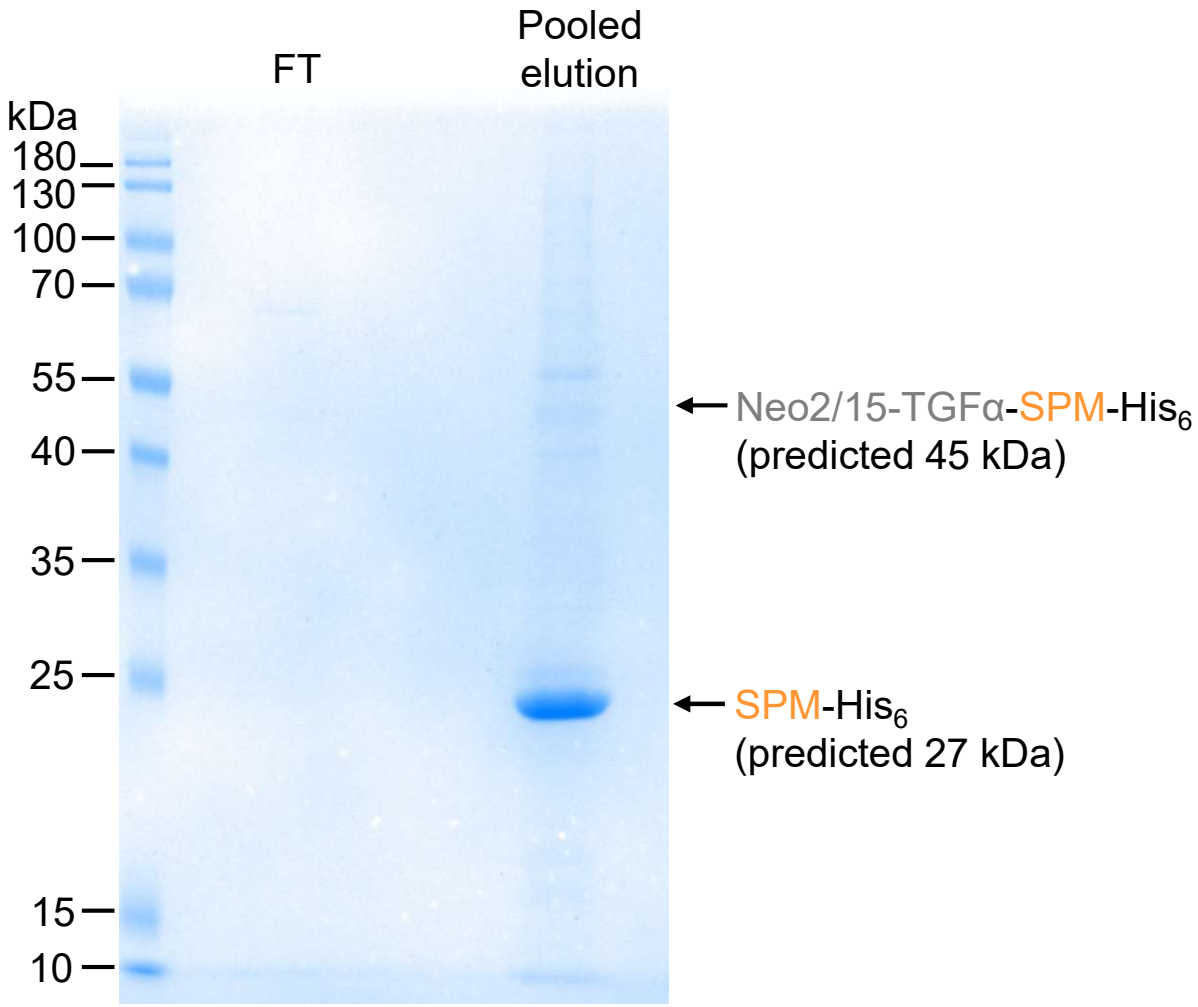

Figure S10: Premature cleavage of Neo2/15-TGFα-SPM-His$_6$ after purification from mammalian cells. Neo2/15-TGFα-SPM-His$_6$ purification from the supernatant of Expi293F cells by nickel-based affinity purification after transient transfection. Fractions are analyzed by SDS-PAGE with Coomassie staining. FT = column flow-through. Minimal full-length Neo2/15-TGFα-SPM-His$_6$ was detected but there was a strong band consistent with the cleaved SPM-His$_6$ product.